TREM2 regulates microglial lipid droplet formation and represses post-ischemic brain injury

Wei Wei [a,1], Lin Zhang [b,1], Wenqiang Xin [a], Yongli Pan [a], Lars Tatenhorst [a], Zhongnan Hao [a], Stefan T. Gerner [c], Sabine Huber [c], Martin Juenemann [c], Marius Butz [d], Hagen B. Huttner [c], Mathias Bähr [a], Dirk Fitzner [a,*], Feng Jia [b,e,**], Thorsten R. Doeppner [a,c,f,g,h,***]

[a] Department of Neurology, University Medical Center Göttingen, Göttingen, Germany
[b] Department of Neurosurgery, Ren Ji Hospital, Shanghai Jiao Tong University School of Medicine, Shanghai, China
[c] Department of Neurology, University of Giessen Medical School, Giessen, Germany
[d] Heart and Brain Research Group, Kerckhoff Heart and Thorax Center, Bad Nauheim, Germany
[e] Department of Neurosurgery, Nantong First People's Hospital, Affiliated Hospital 2 of Nantong University, Nantong, China
[f] Department of Anatomy and Cell Biology, Medical University of Varna, Varna, Bulgaria
[g] Center for Mind, Brain and Behavior (CMBB), University of Marburg and Justus Liebig University Giessen, Giessen, Germany
[h] Research Institute for Health Sciences and Technologies (SABITA), Medipol University, Istanbul, Turkey

ARTICLE INFO

ABSTRACT

Triggering receptor expressed on myeloid cells 2 (TREM2) is a transmembrane receptor protein predominantly expressed in microglia within the central nervous system (CNS). TREM2 regulates multiple microglial functions, including lipid metabolism, immune reaction, inflammation, and microglial phagocytosis. Recent studies have found that TREM2 is highly expressed in activated microglia after ischemic stroke. However, the role of TREM2 in the pathologic response after stroke remains unclear. Herein, TREM2-deficient microglia exhibit an impaired phagocytosis rate and cholesteryl ester (CE) accumulation, leading to lipid droplet formation and upregulation of Perilipin-2 (PLIN2) expression after hypoxia. Knockdown of TREM2 results in increased lipid synthesis (PLIN2, SOAT1) and decreased cholesterol clearance and lipid hydrolysis (LIPA, ApoE, ABCA1, NECH1, and NPC2), further impacting microglial phenotypes. In these lipid droplet-rich microglia, the TGF-β1/Smad2/3 signaling pathway is downregulated, driving microglia towards a pro-inflammatory phenotype. Meanwhile, in a neuron-microglia co-culture system under hypoxic conditions, we found that microglia lost their protective effect against neuronal injury and apoptosis when TREM2 was knocked down. Under in vivo conditions, TREM2 knockdown mice express lower TGF-β1 expression levels and a lower number of anti-inflammatory M2 phenotype microglia, resulting in increased cerebral infarct size, exacerbated neuronal apoptosis, and aggravated neuronal impairment. Our work suggests that TREM2 attenuates stroke-induced neuroinflammation by modulating the TGF-β1/Smad2/3 signaling pathway. TREM2 may play a direct role in the regulation of inflammation and also exert an influence on the post-ischemic inflammation and the stroke pathology progression via regulation of lipid metabolism processes. Thus, underscoring the therapeutic potential of TREM2 agonists in ischemic stroke and making TREM2 an attractive new clinical target for the treatment of ischemic stroke and other inflammation-related diseases.

* Correspondence to: Department of Neurology University of Göttingen Medical School, Göttingen, Germany.
** Correspondence to: Department of Neurosurgery, Ren Ji Hospital, Shanghai Jiao Tong University School of Medicine, No.1630 Dongfang Road, 200127 Shanghai, China.
*** Corresponding author at : Department of Neurology, University of Giessen Medical School, Giessen, Germany.
E-mail addresses: dirk.fitzner@med.uni-goettingen.de (D. Fitzner), projiafeng@163.com (F. Jia), thorsten.doeppner@neuro.med.uni-giessen.de (T.R. Doeppner).
[1] These authors contributed equally to this work.

1. Introduction

Microglia as resident immune cells of the central nervous system (CNS) play a crucial role in the pathophysiology of ischemic stroke [1]. These cells rapidly respond to ischemic stroke by undergoing activation and by releasing various bioactive molecules, such as cytokines, chemokines, and reactive oxygen species (ROS) [2,3]. Whereas the initial activation of microglia is essential for triggering both immune response and tissue repair, dysregulated and excessive microglial activation can exacerbate brain injury and contribute to secondary neuronal damage. Therefore, functional modulation of microglia in ischemic stroke holds great promise for therapeutic interventions with regard to neuroprotection, tissue recovery, and neurological outcome [1,4].

Increasing evidence has shown that modulation of microglial function can help minimize the extent of inflammation and prevent the spread of secondary injury following ischemic stroke [1,5,6]. Triggering receptor expressed on myeloid cells 2 (TREM2), a cell surface receptor expressed on microglia, plays a pivotal role in modulating such microglial function and in maintaining brain homeostasis [7,8]. Current studies suggest that TREM2 is involved in various microglial activities, including phagocytosis, calcium mobilization, energy metabolism, cytokine production, and immune response regulation [8]. Under experimental conditions of either ischemic or hemorrhagic stroke, TREM2 yields neuroprotection and neurological recovery through regulating post-ischemic inflammation and neuronal apoptosis [9–12]. Some of these mechanisms involved in the process affect a regulation of the TLR4 and the PI3K/Akt signaling pathway [13,14].

TREM2 does not exclusively affect the aforementioned TLR4 or PI3K/Akt signaling pathways but rather regulates a plethora of signaling cascades. Indeed, previous reports describe an implication of TREM2 in regulating cholesterol homeostasis and lipid uptake by myeloid cells [15,16]. TREM2 deficient microglia are also associated with altered cholesterol metabolism and impaired lipid clearance [17,18]. Microglia with dysfunctional TREM2 exhibit a reduced ability to phagocyte lipid-rich cellular debris, leading to the accumulation of lipids and the formation of lipid-laden cells [15,19]. In the context of lipid metabolism, activation of TREM2 signaling pathways can enhance the expression of genes involved in lipid uptake, such as scavenger receptors, and promote the clearance of lipid particles. TREM2 also plays a pivotal role in the biogenesis of lipid droplets (LD). It has also been recognized as a lipid sensor within microglia, and the accumulation of LD in aging microglia has been associated with a dysfunctional pro-inflammatory phenotype [20]. In the realm of neurodegenerative diseases, TREM2 has been observed to decrease LD accumulation in aging microglia [21,22]. In contrast, another study found increased expression of TREM2 in chronic cerebral hypoperfusion, and TREM2 knockdown inhibited LD accumulation in microglia, prompting microglial polarization towards an anti-inflammatory and homeostatic phenotype [23]. Therefore, TREM2 regulates LD formation differentially in various diseases, and its neuroprotective role remains controversial. As such, the effect of TREM2 on post-ischemic LD formation remains unclear. Overall, TREM2 plays a critical role in the maintenance of lipid homeostasis and the resolution of innate immune inflammation in microglia [24,25].

Microglial activity, however, is not exclusively regulated by one signaling cascade. As such, the TGF-β1 (Transforming growth factor-beta 1) pathway also plays a significant role in immune response modulation, inflammation regulation, tissue repair, and clearance processes [26,27]. Recent studies in the cancer field have unveiled the impact of TGF-β1 and the TGF-β1/Smad2/3 cellular pathway on lipid metabolism and the genesis of LD [28–31]. In studies focused on breast and lung cancer, TGF-β receptor-mediated pathways can influence cell invasion and lung metastasis by inhibiting LD formation [29,30]. Additionally, in research concerning cancer and bone-related conditions, TGF-β has been found to decrease markers of adipose differentiation and LD formation [28,31], thereby affecting M2 polarization in macrophages [31]. Nevertheless, the specific role of TREM2 in post-ischemic LD formation

of microglia via the TGF-β1/Smad2/3 cellular pathway remains poorly understood. Dysfunction in either TREM2 or TGF-β1 pathways can therefore both impair microglial functions, including phagocytosis of amyloid-beta plaques (Aβ) and clearance of cellular debris, which lead to neuroinflammation and disease progression [8,32,33]. Previous studies report that TREM2 is closely linked to the TGF-β1 signaling pathway in microglia. Hence, TREM2 deficiency results in abnormalities of the TGF-β1 signaling pathway, which in turn triggers abnormal inflammatory responses and apoptosis [34]. Conversely, activation of TREM2 promotes microglia M2 polarization and the release of TGF-β1, which alleviates neuroinflammation and autophagy by activating PI3K/Akt or mTOR signaling [35,36]. In response to TGF-β1, such activated microglia display an increased expression of TREM2 and an increased migratory activity, which facilitates phagocytosis and suppression of secondary neurodegeneration within the peri-infarct tissue [37]. Activated TREM2, in turn, influences TGF-β1 signaling in microglia, presenting a regulatory feedback loop between TREM2 and TGF-β1 that helps maintain immune homeostasis and limit excessive inflammation in the central nervous system [38,39]. A malfunction of this interplay may therefore contribute to secondary brain tissue injury, highlighting the importance of understanding the relationship between TREM2 and TGF-β1 in microglia. The present study therefore analyzes the impact of TREM2 regulation on phenotype and function of microglia under both in vitro and in vivo stroke conditions with a special focus on LD formation and the TGF-β1/Smad2/3 signaling.

2. Materials and methods

2.1. Legal issues, animal housing, randomization and blinding

All animal studies were conducted with local governmental approval according to the protocols of the Institutional Animal Care and Use Committee at Shanghai Jiao Tong University, which were consistent with the National Institutes of Health guidelines and regulations, and following both ARRIVE and STAIR guidelines for the care and use of laboratory animals. Male C57BL/6 J mice aged 10–12 weeks (Vital River Laboratory Animal Technology Co., Beijing, China) were maintained in groups of 5 animals per cage on a regular 12 h light/12 h dark cycle. Throughout the entire stage of the study, all experiments were conducted in a strictly randomized manner. The researchers, possessing local animal experimental licenses, performed animal surgeries and sample collections while maintaining a blinded approach during all study phases. Another researcher was responsible for preparing the experimental solutions and collecting the data. The allocation of solutions and groups was only revealed and disclosed upon completion of the study.

2.2. Cell cultures

All animals for primary cells isolation were kept under 12-hour light/dark circles and received food and water ad libitum. All mice were kept according to the regulations of the European Union (2010/63 EU) in the animal central facility of University Medicine Göttingen (UMG). All experiments were performed in accordance with the animal ethics approval given by the State Authority of Lower Saxony. For all studies, mice were group-housed whenever possible and were randomly assigned to experimental groups. Primary microglia were isolated from newborn pups at postnatal 0–2 days (reproduced by C57Bl/6 J female wild-type mice) [40], obtained from UMG. All cells were tested for potential contamination before the experiment. After the entire brains of the pups were extracted and transferred to a dish filled with cold PBS, the cortex and hippocampus were then delicately isolated. The tissue was digested with 1 mL of 0.25% Trypsin-EDTA and 100 μL of DNAse. Digestion was then terminated with 5 mL of warm primary microglia medium (DMEM-F12 supplemented with 10% FBS and 1% penicillin/streptomycin). After separating microglia from other brain cell

types using density gradient centrifugation, the homogeneous cell suspension was transferred to a T75 flask precoated with poly-L-ornithine (PLO). The culture medium was changed and treated with the murine macrophage colony-stimulating factor (M-CSF, Peprotech, Hamburg, Germany to stimulate microglial proliferation after 5 days. When the microglia have covered the bottom of the flask (about another 5 days), the flask was rigorously shaken to ensure floating of the microglia in the conditioned medium. The primary microglia suspension was seeded at 40,000 cells/cm^2 in PLO-coated dishes or flasks. All primary microglia were passaged 3–4 times to remove astrocytes and neurons before being used in experiments.

Primary cortical neurons were prepared from pregnant C57BL/6 J female mice at embryonic day 16.5 (E16.5), which were sacrificed by CO$_2$ euthanasia [41]. The cerebral cortex and hippocampus were carefully isolated and moved into a 15-mL tube with cold PBS. The tissue at the bottom was digested with 1 mL of 0.25% Trypsin-EDTA and 100 µL of DNAse. Primary neuron culture medium (neurobasal medium supplemented with 2% B27, 1% penicillin/streptomycin, L-glutamine, and additional transferrin) was added to stop the digestion. The medium containing primary neurons was carefully pipetted and centrifuged at 300x g for 5 min, and finally seeded on poly-L-ornithine/laminin (Sigma-Aldrich, Taufkirchen, Germany) pre-coated plates at a density of 200,000 cells/cm^2.

2.3. Oxygen-glucose deprivation (OGD)

The cells were exposed to OGD when the confluence reached 80–90%. Before OGD, cells were washed twice with PBS and incubated with the BSS0 solution (116 mM NaCl, 5.4 mM KCl, 0.8 mM MgSO$_4$, 1 mM NaH$_2$PO$_4$H$_2$O, 26.2 mM NaHCO$_3$, 10 mM HEPES, 0.01 mM glycine and 1.8 mM CaCl$_2$, pH 7.4) and transferred to the hypoxic incubator (Toepffer Lab Systems, Goeppingen, Germany) containing 0.2% O$_2$, 5% CO$_2$ and 70% humidity. After OGD, the BSS0 solution was removed and incubated with the original medium for reoxygenation (RO).

2.4. Primary neuron-microglia co-culture system

The co-culture model used primary microglia and primary neurons to study the effect of microglia on neuron survival under hypoxia conditions. The experiment was based on the protocol of Skaper et al. [42]. Primary microglia were seeded into 6-well (4×10^5 cells/insert) or 24-well (2×10^4 cells/insert) transwells (3 µm pore size; Costar, Maryland, USA). To assess the effect of microglia on neurons under hypoxia, five different microglia species were tested: group 1, microglia with siRNA vehicle under normoxia condition as control; group 2, microglia with negative control siRNA under hypoxia condition; group 3, microglia with siRNA-TREM2 under hypoxia condition; group 4, microglia with negative control siRNA under hypoxia condition plus TGF-β1 receptor inhibitor treatment; group 5, microglia with siRNA-TREM2 under hypoxia condition plus recombinant TGF-β1 treatment. These primary microglia were added to plates pre-seeded with primary neurons, and this co-culture system would be exposed to OGD for 4 h, and incubated for another 48 h RO. Microglia were co-cultured with primary neurons at the start of the OGD of neurons.

2.5. TREM2 siRNA transfection of microglia

Primary microglia were stably transfected with FlexiTube small interfering RNA (siRNA) for mouse TREM2 (NM_018965 target sequence CTTCTGCACTTTGGACATTAA) or negative control siRNA using HiPerFect Transfection Reagent (Qiagen, Hilden, Germany). The siRNA transfection was performed in serum-free medium, following the manufacturer's instruction. The most efficient target sequence for RNA interference was selected from the sequence provided by Qiagen (#SI01455097). All siRNAs were tested for mRNA knockdowns by real-time polymerase chain reaction (PCR). After 24 h of transfection, the cells were used for subsequent experiments.

2.6. Cell viability and cytotoxicity assay

Cell viability was measured via a colorimetric assay by using the MTT (Thiazolyl Blue Tetrazolium Bromide, Sigma-Aldrich, St. Louis, MO) viability assay [43]. After OGD/RO, cell viability was presented as relative changes in percentage compared to normoxic control group. Absorbance was measured with Tecan Sunrise colorimetric microplate reader (Tecan Group AG, Männedorf, Switzerland) at a wavelength of 570 nm. Cytotoxicity was determined by the release of lactate dehydrogenase (LDH) from cells to detect levels of cytotoxicity. A 50 µL aliquot of medium is transferred to another new 96-well plate for each group. An equivalent dose of the test reagent provided by the manufacturer is added to each well to measure the release of LDH from the cells. Measure the optical absorbance at a wavelength of 490 nm.

2.7. Middle cerebral artery occlusion (MCAO) and animal groups

For induction of ischemic stroke in mice, the middle cerebral artery occlusion (MCAO) model based on our previous study was used [44]. Male C57BL/6 J mice (aged 10–12 weeks) were anesthetized with 3% isoflurane at the beginning of surgery and maintained with 2.5% during surgery. After sterilization and analgesia of the mice, a 1 cm incision was carefully incised to expose the right common carotid artery (CCA). A silicon-coated microfilament was inserted into the right CCA and was slowly pushed forward to the right middle cerebral artery (MCA) to block blood flow. Laser Speckle Imaging System (LSIS, RWD Life Science, Shenzhen, Guangdong, China) was applied to ensure successful blood flow block and cerebral blood flow parameters were recorded. After 60 min, the microfilament was removed for reperfusion. The experimental paradigm design and cerebral blood flow parameters of LSIS are shown in Supplementary Fig. S1. The survival rate of each group of mice used in the experiment are shown in Supplementary Table 1.

2.8. TREM2 siRNA transfection of mice in vivo

Mice were placed in a stereotaxic locator (Wuhan Yihong Technology Co., Ltd., Wuhan, China) 10 min after successful establishment of the MCAO model as previously described [26,27]. Each mouse received 3 µL of a mixture of TREM2-siRNA (Qiagen, Shanghai, China) and control siRNA (1.8 µL control siRNA, 0.8 µL RNA-Mate, 0.4 µL ddH$_2$O). The liquid was slowly injected into the lateral ventricles at a rate of 0.5 µL/min via a mini-pump (RWD, Shenzhen, China).

2.9. 2,3,5-Triphenyltetrazolium chloride (TTC) staining

Brains were dissociated and cut into 2 mm thick coronal sections, 2 mm sections were incubated with 2% TTC solution for 30 min at 37 °C in the dark, and the staining process was stopped with 4% paraformaldehyde in PBS. The infarct proportion was calculated by the formula: corrected percentage of infarct volume = (contralateral hemispheric volume – ipsilateral non-infarcted volume) / contralateral hemispheric volume x 100%.

2.10. Immunohistochemistry and immunocytochemistry staining

Primary microglia were seeded on PLO-coated chambers at a density of 4×10^4/cm^2. Cells were washed once with cold PBS and then fixed in 4% paraformaldehyde (PFA) for 20 min. The cells were washed three times with PBS, then permeabilized with 0.25% Triton X-100 for 15 min and blocking at room temperature for 1 h. After the incubation of primary antibodies (Iba1, CD68, CD11b, TMEM119, NeuN, CD206, GFAP, and CX3CR1) overnight, the slides were incubated with the corresponding secondary antibody for 2 h or with BODIPY 493/503 for 30

min. For in vivo tissue staining, post-perfusion brain samples from C57BL/6 J mice were fixed in 4% PFA for 24 h, dehydrated with 30% sucrose, and prepared into 14 μm tissue sections with a cryostat. Cryosections were incubated with citrate solution for antigen retrieval, followed by 1 h of blocking at room temperature. Sections were incubated overnight with the following primary antibodies: Iba1, CD68, and CD206. After primary antibody incubation, sections were washed three times in TBS, the following secondary antibodies were incubated at room temperature for 2 h (RT). Then the sections were washed three times in TBS. Nuclei staining was then performed with 4',6-Diamidin-2-phenylindol (DAPI, 1:10,000; AppliChem, Darmstadt, Germany). Finally, Vectashield (Vector Laboratories, H-1000) was used for mounting. Specific antibody working concentrations are shown in Supplementary Table 2.

2.11. Apoptosis TUNEL staining assay

Terminal deoxynucleotidyl transferase dUTP nick end labeling (TUNEL, in situ cell death detection kit, Sigma-aldrich) staining was used to detect cell death according to the manufacturer's instructions. After specific treatment, cells were fixed and permeabilized. Subsequently, working reaction mixture was prepared with 50 μL total volume of Enzyme solution into 450 μL label solution to obtain 500 μL TUNEL reaction mixture. Then the cells were incubated with the TUNEL reaction mixture for 1 h at 37 °C in the dark. Afterward, DAPI staining is used to stain cell nuclei.

2.12. Quantitative analysis of immunofluorescence data

The cortex and striatum were detected as regions of interest (ROI), five randomly selected fields of view per overlay were photographed, and three images were taken for each region. The average neuron or microglia density was determined for all ROIs. For cell slides in vitro, photographs were taken in 3 fields of view. Each overlay was randomly selected. Immunofluorescence slides were photographed with a Zeiss Axioplan 2 fluorescence microscope (Zeiss, Oberkochen, Germany) or confocal scanning laser microscope (Zeiss LSM 700, Zeiss, Germany). Images were processed with ZEN software version 3.20. Cell colocalization analysis and fluorescence intensity quantification were performed with ImageJ software version 1.60.

2.13. Western blotting analysis

The brain tissue samples and the cell samples were lysed in a solution buffer containing RIPA Lysis and Extraction Buffer (Thermo Scientific, Waltham, USA), 1 mmol/L EDTA, 1% protease inhibitor, and 1% phosphatase inhibitor with a homogenisator or sonicator for 10 min and subsequently centrifuged at 4 °C with 14,000 rpm for 15 min. Protein concentrations were quantified with the Pierce BCA protein assay kit (Thermo Fisher Scientific, USA). Equal amounts of protein were loaded on 8–12% SDS-PAGE gel and electrophoretically separated in sample buffer (dithiothreitol, final 0.1 M concentration, 0.1% SDS, 0.1 M Tris HCl; pH 7.0). The electrophoresis gel was transferred to a polyvinylidene fluoride membrane (Merck Group, Darmstadt, Germany) by the tank transfer protocol. The membranes were then incubated in blocking buffer for 1 h at room temperature, followed by overnight incubation for optimal results with primary antibodies: TREM2, TGF-β1, p-Smad 2/3, Smad 2/3, PLIN2, BAX, Bcl-2, and GAPDH. After three times washes with TBS-T, the blots were incubated with secondary antibodies (1:10,000) for 1 h. Specific antibody working dilutions are given in the Supplementary Table 2. ImageJ version 1.60 was used to measure the grey value of each blot.

2.14. Quantitative real-time polymerase chain reaction (qRT-PCR)

To extract total RNA, TRIzol (Invitrogen, Darmstadt, Germany) was used according to the manufacturer's instructions. The total RNA concentration was determined with a NanoDrop ND1000 Spectrophotometer (NanoDrop, Wilmington, DE, USA). The mRNA was reversely transcribed to cDNA with the RevertAid H Minus First Strand cDNA Synthesis Kit, followed by qRT-PCR with the SYBR Green I Master Kit for LightCycler® 480 (Merck Group) according to the manufacturer's instructions. All PCR primers were purchased from Eurofins Genomics (Luxembourg, Germany). The sequences of all primers are shown in Supplementary Table 3. The relative expression levels were calculated and quantified using the $2^{-\Delta\Delta CT}$ method after normalization with the reference β-actin. The reported results are based on at least three independent experiments performed on different batches of cells or mice.

2.15. Enzyme linked immunosorbent assay (ELISA)

Concentrations of TGF-β1 were determined with commercial ELISA kits (Thermo Fisher Scientific, USA) according to the manufacturer's instructions. A 96-well plate was coated with capture antibody at 100 μL/well. The plate was then sealed and incubated overnight at 4 °C. The wells were blocked with 200 μL ELISA/elispot diluent for 1 h of incubation. Standard samples were prepared as instruction for a standard curve, and 100 μL/well of diluted detection antibody was added to each well and incubated for 1 h. After aspirating and 3–5 times washing, 100 μL/well of diluted horseradish (avidin-HRP) was added to each well and incubated at room temperature for 30 min. The absorbance of the samples was detected at 450 nm by the colorimetric reader.

2.16. Quantification of total cholesterol, free cholesterol, and cholesteryl ester

Total cholesterol, free cholesterol, and cholesteryl ester in tissue or cell samples were analyzed by commercially available cholesterol quantification kits (Abcam, ab65359, Germany). For generating a standard curve, the standard solution was diluted into 25 μL of different proportions to prepare six sets of standard samples. Testing samples were divided into two reaction mixtures, i.e., with or without cholesterol esterase. Total cholesterol and free cholesterol were measured separately, and added to appropriate wells of a 96-well plate. Reagent and enzyme mix were mixed thoroughly as a reaction buffer according to the commercial instruction. Samples were mixed with reaction buffer and incubated at 37 °C for 60 min in the dark. The fluorescence value was measured at exc/em = 535/587 nm with a fluorometric microplate reader and normalized with the standard curve.

2.17. Flow cytometry analysis

CD206 + M2 microglia in the cerebral hemisphere after MCAO were determined by flow cytometry with a fluorescence-activated cell sorter. Ischemic cerebral hemispheres were mechanically homogenized in lysis buffer (0.5% BSA, 5% glucose, 10 mg/mL DNase in PBS) and centrifuged at 1600 rpm for 10 min. Thereafter, the pellets were dissolved in a 30% Percoll solution (GE Healthcare, USA) and loaded onto a gradient containing 45% and 70% Percoll. After centrifugation, the cells were aspirated between stages and dissolved in working solution (3% fetal bovine serum in PBS). Before antibody labeling, the cell suspension was incubated with anti-mouse Fc-Block (final concentration of 2.5 μg/mL) for 10 min at 4 °C to prevent non-specific binding. After washing, cells were incubated with anti-CD45, anti-CD11b and anti-CD206 (BioLegend, San Diego, USA) overnight. Flow cytometry quantification was obtained using FlowJo v. 10.8.1 (BD FACSDiva™) software.

2.18. In vitro phagocytosis assay

For in vitro phagocytosis assays, primary microglia were seeded on 96-well plates (1 ×10⁴ cells/well) and incubated in the cell culture medium and treated with various conditions for 24 h. Following specific

treatments, 5 ng of pHRodo Red Zymosan Bioparticles (Thermo Fisher Scientific, P35364) were dissolved in the cell culture medium according to the instruction of the supplier. Cells were incubated with or without Zymosan Bioparticles for 4 h. In order to extinguish the signal interference of the extracellular fluorescent bioparticles, cells were washed with 0.25 mg/mL trypan blue in PBS for one time. After cells were subsequently lysed with 1% PBS-Triton, the samples were analyzed using a fluorescence plate reader (560 nm excitation wavelength and 585 nm emission wavelength). To acquire images of phagocytosis, microglia were seeded on 4-well chambers (4×10^4 cells/well, Sarstedt, Germany). pHRodo Red Zymosan Bioparticles were added as described above. The cells were then washed two times with PBS before fixation and permeabilization, then incubated with specific primary and secondary antibodies. Nuclei were stained with DAPI. Immunofluorescence slides were photographed with Zeiss Axioplan 2 fluorescence microscope (Zeiss, Oberkochen, Germany).

2.19. Analysis of post-stroke motor coordination deficits

In the tests for the analysis of motor coordination in mice, the rotarod test, the tightrope test, the balance beam test, and the corner turn test were performed at the time points given (pre-ischemia day 1; post-ischemia day 2, 5 and 7) [45]. Mice were trained on days 1 and 2 prior to the MCAO surgery to ensure correct test behavior as previously reported [46–49]. The rotarod, the balance beam and the tightrope walking tests were performed for three individual tests, and the mean was calculated thereafter. For the rotarod test, the recorded parameter was the time until the mice fell off, with a maximum test time of 300 s. Details of the scoring sheet for the tightrope test can be found in the Supplementary Table 4. The corner turn test consisted of 10 trials per test day, during which the lateral index (number of right turns per 10 trials) was calculated, with a high lateral index close to a score of 1 indicating severe motor coordination deficits.

2.20. Statistical Analysis

For comparison of two groups, the two-tailed independent Student's t-test was used. For comparison of three or more groups, a one-way analysis of variance (ANOVA) followed by Tukey's post-hoc-test, and if appropriate, a two-way ANOVA was used. The effect size was 0.3. Unless otherwise stated, data are presented as means with SD values. A p-value of < 0.05 was considered statistically significant. Statistical software was Graphpad Prism version 8.0.

3. Results

3.1. Oxygen-glucose deprivation (OGD) induces an upregulation of TREM2 expression in primary microglia

The purity and characteristics of the extracted primary microglia cultures were characterized by phase contrast microscopy and staining for microglial markers: Iba1, CD11b, CX3CR1, and TMEM119 (Supplementary Fig. S2A). To determine the optimal OGD duration, primary microglia and neurons were exposed to different OGD times (2 h, 4 h, 6 h, and 8 h). We found 4 h of OGD as the ideal duration, resulting in a cell viability of 50% for microglia and neuronal cells (Supplementary Fig. S2B-D). We then identified the cell types in which TREM2 was increased following exposure to hypoxia. We selected the microglia marker Iba-1, the astrocyte marker GFAP, and the neuronal marker NeuN. By immunofluorescence co-localization staining analysis of TREM2, we found that TREM2 was predominantly expressed in microglia but not in astrocytes or neurons (Fig. 1A). Furthermore, we examined changes in TREM2 expression in microglia at protein levels after hypoxia by Western blotting and found that TREM2 expression significantly peaked after 4 h of OGD and subsequently decreased (Fig. 1B). Interestingly, the increase in protein abundance of TREM2 depended on

the duration of RO (12 h, 24 h, and 48 h), which in turn correlated with the extent of cell injury (Fig. 1C). Immunocytochemistry staining revealed increased patterns of M2 polarization of microglia exposed to 4 h of OGD with different RO times of 24 h or 48 h, respectively, as indicated by co-staining against Iba1 and CD206 (Fig. 1D).

3.2. TREM2 upregulates TGF-β1 expression activating the TGF-β1/Smad2/3 pathway

Western blotting regarding TGF-β1 expression in microglia exposed to hypoxia displayed a similar temporal resolution pattern as seen for TREM2. As such, TGF-β1 expression peaked at 4 h of OGD (Fig. 2A) and increased even further depending on the duration of RO (12 h, 24 h, and 48 h) (Fig. 2B). To further validate the regulation of microglial function by TREM2 through the TGF-β1/Smad2/3 signaling pathway, we knock downed TREM2 and validated the knockdown efficiency both at the mRNA level (Supplementary Fig. S3A) and at the protein level (Supplementary Fig. S3B, C). Designing a neuron/microglia co-culture system, the impact of TREM2-silenced microglia on neuronal survival after OGD was analyzed (Fig. 2C). When primary microglia were exposed to OGD, both TGF-β1 (Fig. 2D) and p-Smad2/3 (Fig. 2E) protein levels were significantly upregulated. In contrast, p-Smad2/3 and TGF-β1 expression were reduced in the si-TREM2 group. The application of recombinant TGF-β1 (rTGF-β1), in turn, reversed the effect of si-TREM2-induced down-regulation of both p-Smad2/3 and TGF-β1. Neither rTGF-β1 nor TGF-β1 receptor inhibitor treatment, however, affected TREM2 protein levels themselves (Supplementary Fig. S3D).

3.3. OGD induces upregulation of TREM2 associated with changed cholesterol levels and microglial activity

We further examined the role of TREM2 in post-hypoxic microglia with regard to morphology and functional activity. We found that mRNA levels of CD206, TGF-β1, PLIN2, and TNF-α were significantly upregulated upon induction of OGD/RO. When TREM2 was silenced, mRNA levels of the inflammatory factor TNF-α and the LD marker PLIN2 were increased, whereas levels of the M2 phenotype marker CD206 and the anti-inflammatory factor TGF-β1 were reduced. The latter was reversed by ectopic rTGF-β1 treatment (Fig. 3A-D). ELISA assays confirmed the aforementioned PCR results, i.e., protein levels were in line with mRNA levels (Fig. 3E). Further experiments focused on an analysis of microglial lipid patterns after regulation of TREM2. The mRNA levels of several lipid metabolism-related genes (LMRG) were significantly upregulated after induction of OGD/RO. When TREM2 was knocked down, lipid and cholesterol synthesis was elevated (upregulation of PLIN2 and SOAT), whereas with impaired cholesterol clearance and lipid transport (downregulation of ApoE, ABCA1, and NPC2) lipid hydrolysis was impaired (downregulation of LIPA and NCEH). Unlike previous inflammatory genes, using rTGF-β1 did not alter the LMRG mRNA levels (Supplementary Fig. S4A-G). Total cholesterol (TC), free cholesterol (FC) and cholesteryl esters (CE) were increased in microglia exposed to OGD. Silencing TREM2 increased these three lipids forms even further, whereas ectopic rTGF-β1 reversed these effects. The TGF-β1 inhibitor, on the contrary, had no significant effect in this respect (Fig. 3F-H). In line with this, silencing of TREM2 induced an upregulation of PLIN2 on the protein level (Fig. 3I). A co-localization staining analysis of a LD marker (BODIPY) and the M2 microglia marker CD206 revealed that knockdown of TREM2 significantly elevated microglial LD aggregation and reduced the number of M2 microglia (CD206 +). This trend was exacerbated by TGF-β1 inhibitor treatment, an observation that was reversed by rTGF-β1 treatment. Interestingly, BODIPY+ microglia with large amounts of LDs failed to co-localize with the CD206 marker (Fig. 3J-L). These data suggest that TREM2 may play an inhibitory role for regulating post-hypoxic inflammatory responses of cultured microglia.
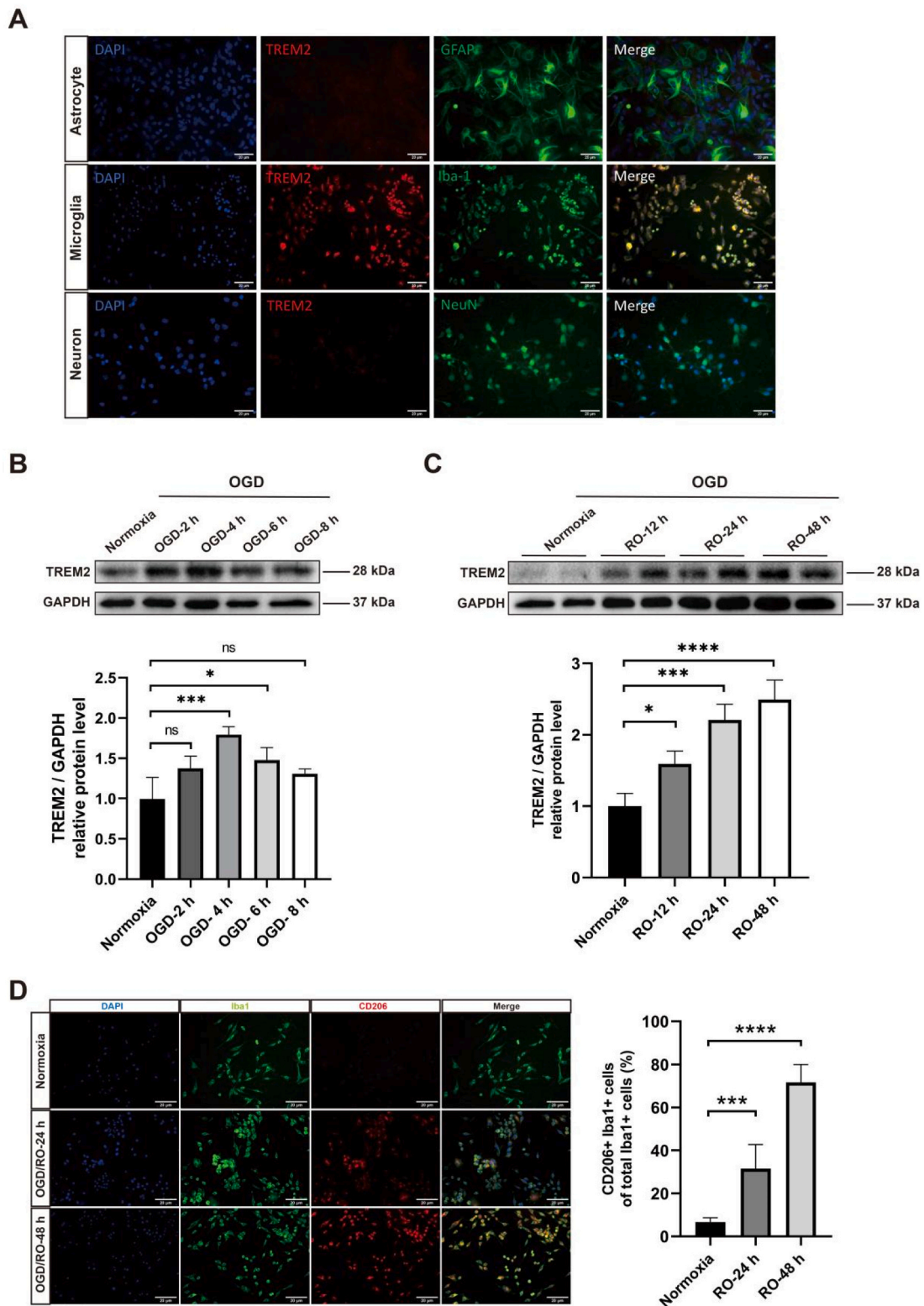
Fig. 1. Oxygen-glucose deprivation (OGD) induces upregulation of the expression of TREM2 and stimulates M2 polarization in primary microglia. A Immunofluorescence staining of TREM2 (red) expression of astrocytes, microglia, and neurons (green) in normoxia conditions. **B** Quantitative analysis of TREM2 expression of microglia exposed to different hypoxia times (2 h, 4 h, 6 h, 8 h, normoxia as control group) using Western blot analysis normalized with the housekeeping protein GAPDH (n = 3). **C** Quantitative analysis of TREM2 expression of microglia after 4 h of hypoxia following different reoxygenation times (RO, 12 h, 24 h, 48 h, normoxia as control group) using Western blot analysis normalized with the housekeeping protein GAPDH (n = 3). **D** Immunofluorescence staining of M2 microglia (CD206 +, red) with regard to the dynamic change after hypoxia. The data are quantified as percentage of M2 microglia of total microglia (Iba1 +, n = 5). Statistical tests: Data are expressed as mean ± SD, NS: no significance, *p < 0.05, * *p < 0.01, * **p < 0.001, * ** *p < 0.0001. Scale bars, 20 μm (A) and (D). Abbreviation: TREM2, Triggering Receptor Expressed on Myeloid Cells 2; OGD, oxygen-glucose deprivation; RO, reoxygenation.
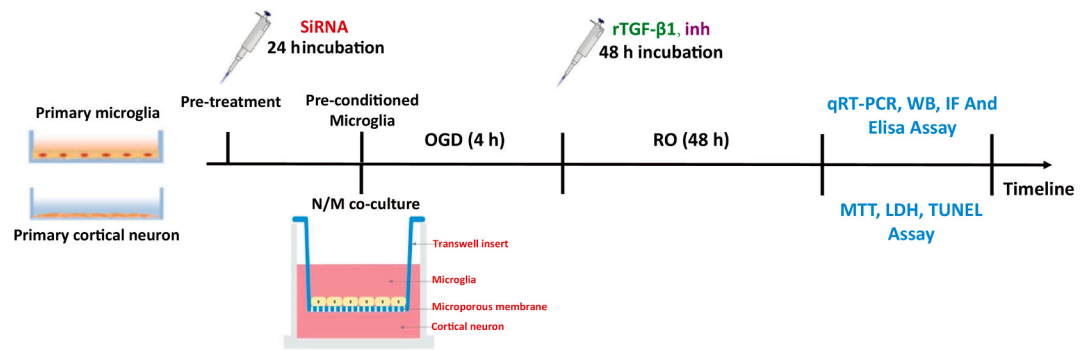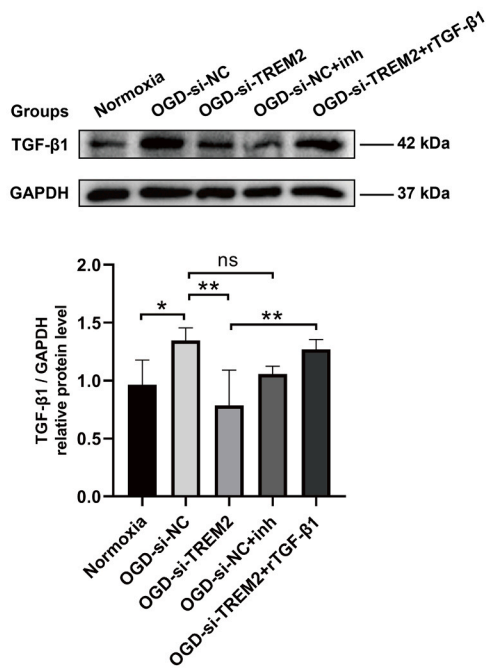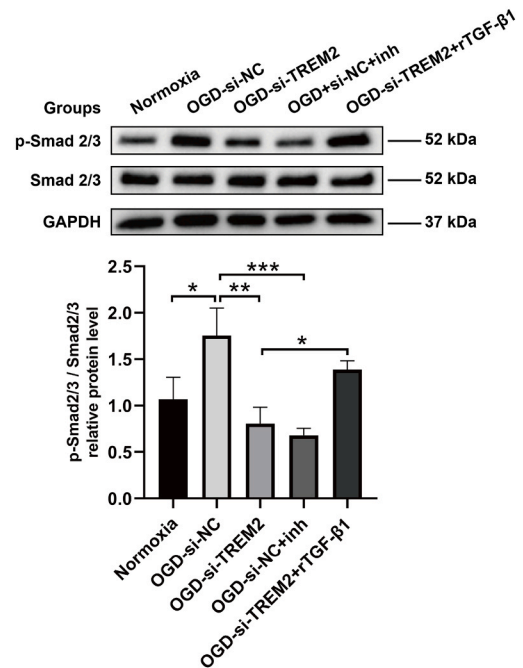
A
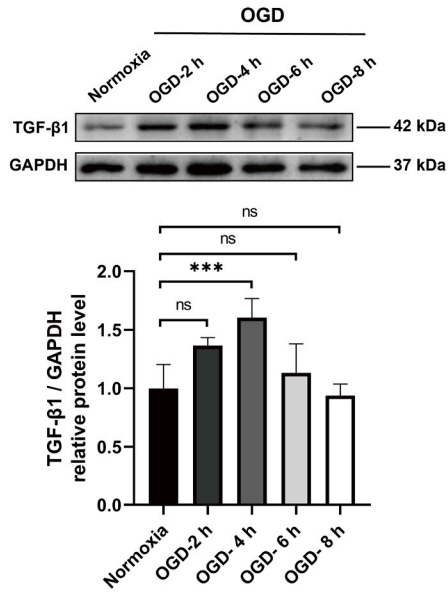
B
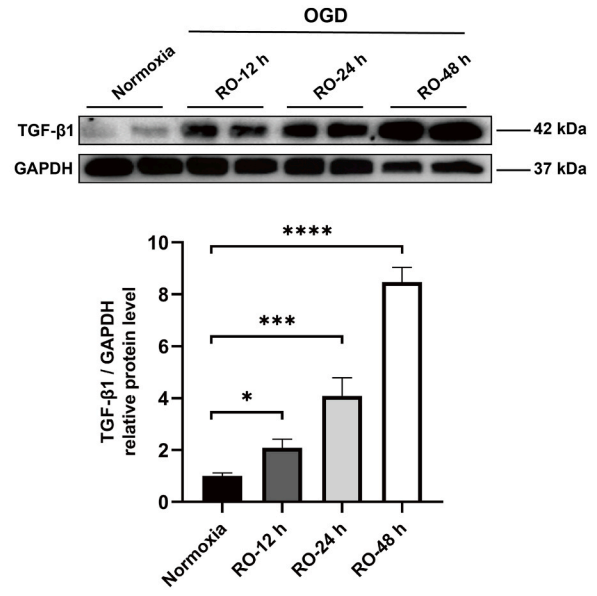
C

D

E

(caption on next page)

Fig. 2. Silencing of TREM2 in primary microglia downregulates the expression of TGF-β1 and p-Smad2/3 after hypoxia. **A** Quantitative analysis of TGF-β1 expression of microglia exposed to different hypoxia times (2 h, 4 h, 6 h, 8 h, normoxia as control group) using Western blot analysis normalized with the housekeeping protein GAPDH (n = 3). **B** Quantitative analysis of TGF-β1 expression of microglia after 4 h of hypoxia following different reoxygenation times (RO, 12 h, 24 h. 48 h, normoxia as control group) using Western blot analysis normalized with the housekeeping protein GAPDH (n = 3). **C** Schematic diagram of the siRNA-TREM2 treatment of microglia and the microglia/neuron co-culture system: Primary microglia were treated with siRNA-TREM2 knockdown 24 h before co-culture with neurons. After OGD/RO, microglia were used for ELISA, phagocytosis efficiency, PCR and Western blotting assays. Neurons were used for MTT cell survival assays, LDH cytotoxicity release assays, and apoptosis assays, respectively. **D** Quantitative analysis of p-Smad2/3 and Smad2/3 expression in microglia using Western blot analysis normalized with the housekeeping protein GAPDH in five groups: group 1 (normoxia as control group); group 2 (OGD/RO treatment with siRNA solvent); group 3 (10 nM siRNA-TREM2 with 24 h incubation before OGD/RO); group 4 (2 μM TGF-β1 receptor inhibitor treatment in group 2); group 5 (10 ng/mL re-combinant TGF-β1 treatment in group 3) (n = 3). **E** Quantitative analysis of TGF-β1 expression in microglia using Western blot analysis normalized with the housekeeping protein GAPDH in the five groups mentioned above (n = 3). Statistical tests: Data are expressed as mean ± SD, *p < 0.05, * *p < 0.01, * **p < 0.001, and * ** *p < 0.0001. Abbreviation: TGF-β1, Transforming growth factor beta 1; OGD, oxygen-glucose deprivation; RO, reoxygenation; siRNA, small interfering RNA; si-TREM2, TREM2 siRNA; inh, TGF-β1 receptor inhibitor; rTGF-β1, recombinant TGF-β1; IF, Immunofluorescence staining; WB, Western blotting assay; LDH, lactate dehydrogenase.

3.4. TREM2 affects phagocytosis of microglia after hypoxia

We also investigated whether or not TREM2 modulates phagocytosis of microglia under the same conditions as reported before. In cultured primary microglia, OGD stimulation resulted in a slight increase in the number of phagocytic Zymosan particles in activated microglia (no statistical significance), whereas treatment with siRNA-TREM2 signifi-cantly reduced phagocytosis in comparison to OGD conditions (Fig. 4A-B). Of note, rTGF-β1 treatment partially restored phagocytosis in TREM2-silenced microglia. No effect was observed when primary microglia were treated with the TGF-β1 inhibitor compared to the nor-moxia group. In addition, phagocytosis efficiency was also measured by detecting the fluorescence intensity of Zymosan Bioparticles (Fig. 4C). Such an experimental approach demonstrated that silencing of TREM2 inhibits phagocytosis of microglia after OGD, which is consistent with previous results from the fluorescent staining. Thus, TREM2 appears to regulate phagocytosis independent of the TGF-β1 receptor-mediated signaling pathway.

3.5. TREM2 enhances neuroprotective properties of co-cultured microglia under hypoxia conditions

In a co-culture system of primary cortical neurons and microglia under OGD conditions, we found that TREM2-silenced microglia lost their neuroprotective effects, and neurons co-cultured with them showed decreased survival, reduced cell viability, and elevated cyto-toxicity compared to controls (Fig. 5A-B). To determine whether the microglial TREM2 affects neuronal hypoxic injury via the TGF-β1/Smad2/3 pathway, we counteracted the effects of TGF-β1 on p-Smad2/3 signaling using the TGF-β1 receptor inhibitor. As expected, such an experimental approach resulted in a most severe neuronal cell injury. Administration of rTGF-β1 activated the TGF-β1/Smad2/3 pathway, reversing the damaging effect of silencing TREM2 due to si-TREM2 treatment alone. Likewise, TUNEL staining used in the five experi-mental groups described above revealed that si-NC-treated microglia but not si-TREM2-silenced microglia significantly reduced neuronal apoptotic damage (Fig. 5C-D). Such results were confirmed by analyzing the expression of the pro-apoptotic protein BAX and the anti-apoptotic protein Bcl-2 in hypoxic neurons (Fig. 5E-F). TREM2 reduced apoptotic signaling in hypoxic neurons via the TGF-β1/Smad2/3 pathway, whereas application of the TGF-β1 receptor inhibitor or the si-TREM2 reversed this effect. This data suggests that TREM2 may be a key player involved in regulating the neuronal protective effects of microglia.

3.6. TREM2 regulates microglial morphology and activity via the TGF-β1/smad2/3 pathway under in vivo stroke conditions

To study the role of TREM2 in regulating the TGF-β1/Smad2/3 pathway in microglia responding to ischemic stroke, we analyzed TGF-β1, p-Smad2/3 and Smad2/3 protein expression in mice subjected to

60 min of MCAO. Firstly, TREM2 was knocked down using the optimal and safest si-TREM2 dose and concentration (3 μL, 2 nM, injected in 3 min). Both PCR and Western blot assays confirmed a successful knockdown of TREM2 in mice (Supplementary Fig. S5A-C). Samples from the ischemic hemisphere showed that both TGF-β1 protein levels and the p-Smad2/3/Smad2/3 expression ratio were increased in the MCAO+si-NC control group, whereas a significant decrease was observed in the si-TREM2 knockdown group. The latter was reversed by rTGF-β1 treatment (Fig. 6A-B). However, PLIN2 expression showed a significant upregulation in the TREM2 knockdown group, exhibiting an opposite trend to TGF-β1 (Fig. 6C). In line with this, mRNA levels of CD206, TGF-β1, PLIN2 and TNF-α were all differentially upregulated after MCAO. Following the knockdown of TREM2, mRNA levels of the inflammatory factors TNF-α and PLIN2 were further increased, whereas levels of the M2 phenotypic marker CD206 and the anti-inflammatory factor TGF-β1 were reduced and could be reversed by rTGF-β1 treat-ment (Fig. 6D-G). Parallel to the results of the in vitro experiments, the knockdown of TREM2 led to elevated lipid and cholesterol synthesis alongside an impaired cholesterol clearance and lipid transport. Nevertheless, alterations in LIPA and NCEH1, the regulators of lipid hydrolysis, did not exhibit significant changes. Additionally, rTGF-β1 demonstrated a down-regulation in the LD formation and cholesterol synthesis (PLIN2 and SOAT1). However, it did not significantly affect the mRNA levels of other LMRGs in MCAO mice (Supplementary Fig. S6A-G). The immunofluorescence staining analysis of ischemic hemispheres revealed that TREM2 knockdown significantly reduced the number of M2 phenotype (CD206 +) microglia and significantly increased the number of M1 phenotype (iNOS+) microglia when compared to the MCAO+si-NC control group. Likewise, rTGF-β1 treat-ment in si-TREM2 knockdown MCAO mice showed an increased number of M2 polarized microglia within the ischemic hemisphere (Fig. 6H-J). These in vivo results suggest that TREM2 may be a critical key player in regulating PLIN2 expression, lipid accumulation and TGF-β1/Smad2/3 pathway activation in residing microglia of ischemic hemispheres.

3.7. TREM2 reduces post-stroke brain injury in mice

Based on our above findings, we further investigated whether or not TREM2 knockdown affects apoptosis and infarct size in the post-ischemic brain. Analyzing infarct volumes at day 7 post-ischemia revealed that TREM2 knockdown resulted in increased brain infarcts compared to the si-NC control group. Application of rTGF-β1, in contrast, attenuated brain injury in the TREM2 knockdown mice (Fig. 7A-B). Likewise, BAX/Bcl-2 ratios were significantly increased after TREM2 knockdown, whereas rTGF-β1 reversed this effect (Fig. 7C-D). The TUNEL staining experiments confirmed the aforementioned results with regard to the extent of post-stroke brain injury in the different experimental groups (Fig. 7E-F).
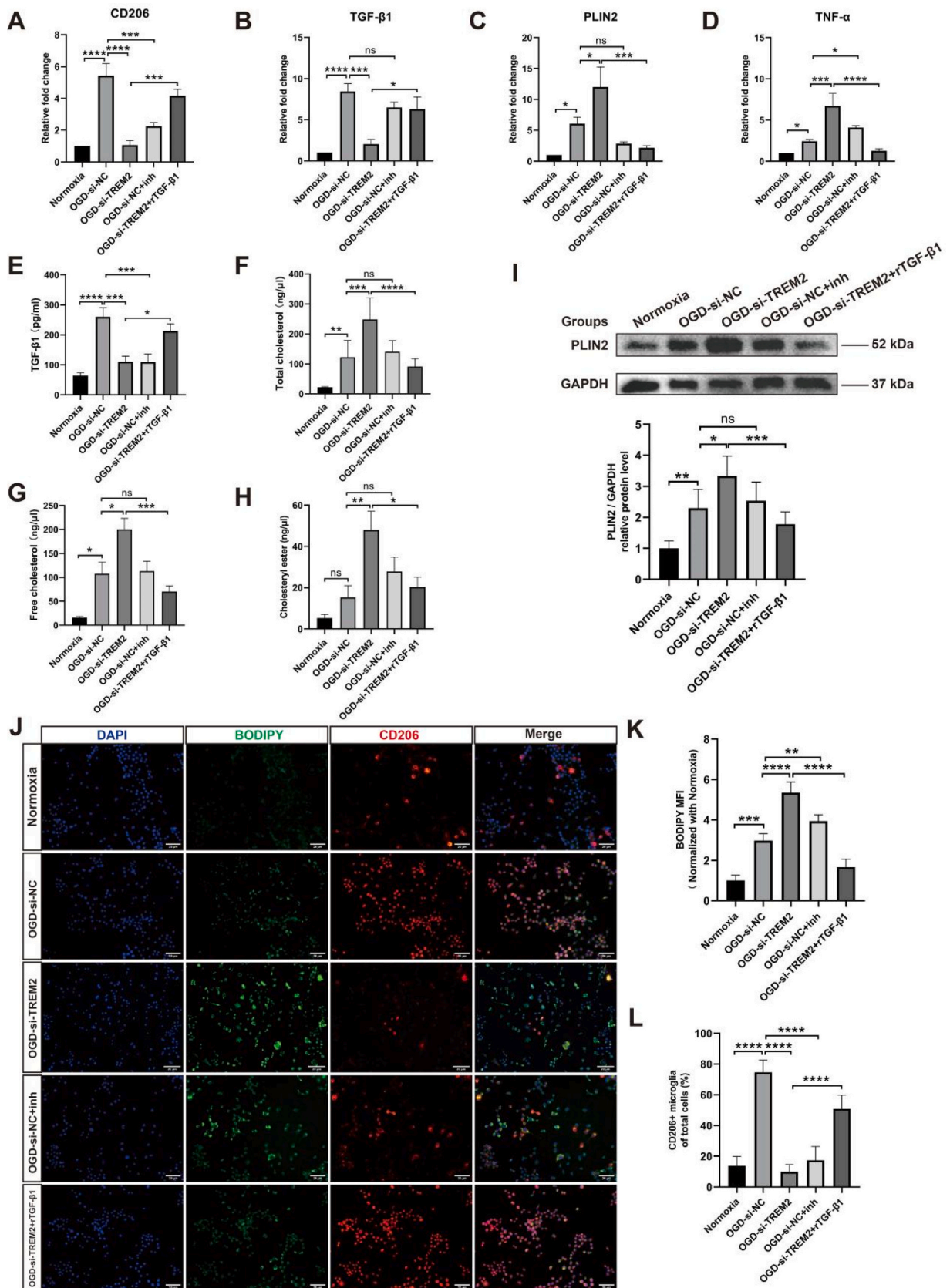
(caption on next page)

Fig. 3. OGD induces the upregulation of TREM2, alters cholesterol levels, and regulates the polarization phenotype and inflammatory factor levels of microglia. A-D Quantitative analysis of CD206 (A), TGF-β1 (B), PLIN2 (C), and TNF-α (D) mRNA expression in primary microglia using quantitative real-time polymerase chain reaction (qRT-PCR) normalized with the housekeeping gene β-actin (n = 5). E For cytokine quantification, we measured the production of TGF-β1 by using an Enzyme-linked immunosorbent assay (ELISA) in the same five groups (n = 5). F-H Quantification of the level of total cholesterol (F), free cholesterol (G), and cholesteryl ester (H) in the same five groups (n = 5). I Quantitative analysis of PLIN2 expression in microglia using Western blot analysis normalized with the housekeeping protein GAPDH in the five groups mentioned above (n = 3). J Immunofluorescence co-staining of lipid droplets (LD, BODIPY, green) and M2 polarization of primary microglia (CD206, red) in the aforementioned 5 groups. K Quantification of the percentage of CD206 + microglia of total microglia (Iba1 +, n = 5). L Quantitative analysis of the mean fluorescence intensity (MFI) of BODIPY (n = 5). Statistical tests: Data are expressed as mean ± SD, NS: no significance, *p < 0.05, * *p < 0.01, * **p < 0.001, * ** *p < 0.0001. Scale bars, 20 μm (J). Abbreviation: TGF-β1, Transforming growth factor beta 1; PLIN2, Perilipin 2; TNF-α, Tumor necrosis factor alpha; OGD, oxygen-glucose deprivation; RO, reoxygenation; si-TREM2, TREM2 siRNA; inh, TGF-β1 receptor inhibitor; rTGF-β1, recombinant TGF-β1; qRT-PCR, quantitative real-time polymerase chain reaction; ELISA, Enzyme-linked immunosorbent assay; LD, lipid droplets; MFI, mean fluorescence intensity.
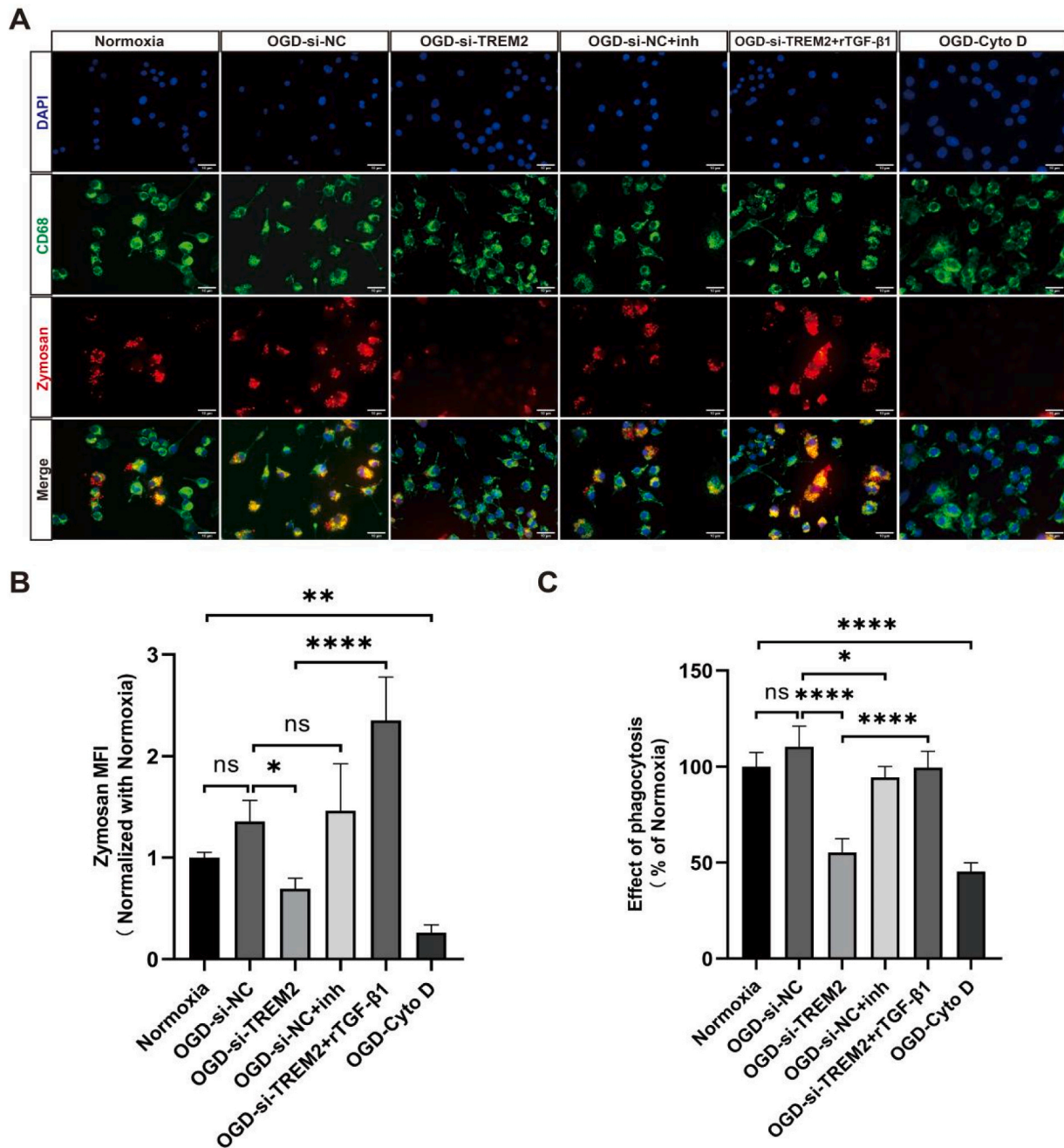

Fig. 4. TREM2 enhances phagocytosis of microglia after hypoxia. A Immunofluorescence staining of CD68 (green) and Zymosan Bioparticles (red) in microglia in the aforementioned 5 groups and the Cytochalasin D treated group as a positive control. B Quantification of the mean fluorescence intensity (MFI) of Zymosan Bioparticles in microglia (n = 5). C Quantitative analysis of phagocytosis efficiency in microglia in the aforementioned 6 groups using quantitative fluorometric assay. Statistical tests: Data are expressed as mean ± SD, NS: no significance, *p < 0.05, * ** *p < 0.0001. Scale bars, 10 μm (A). Abbreviation: OGD, oxygen-glucose deprivation; MFI, mean fluorescence intensity; si-TREM2, TREM2 siRNA; inh, TGF-β1 receptor inhibitor; rTGF-β1, recombinant TGF-β1; Cyto D, Cytochalasin D.
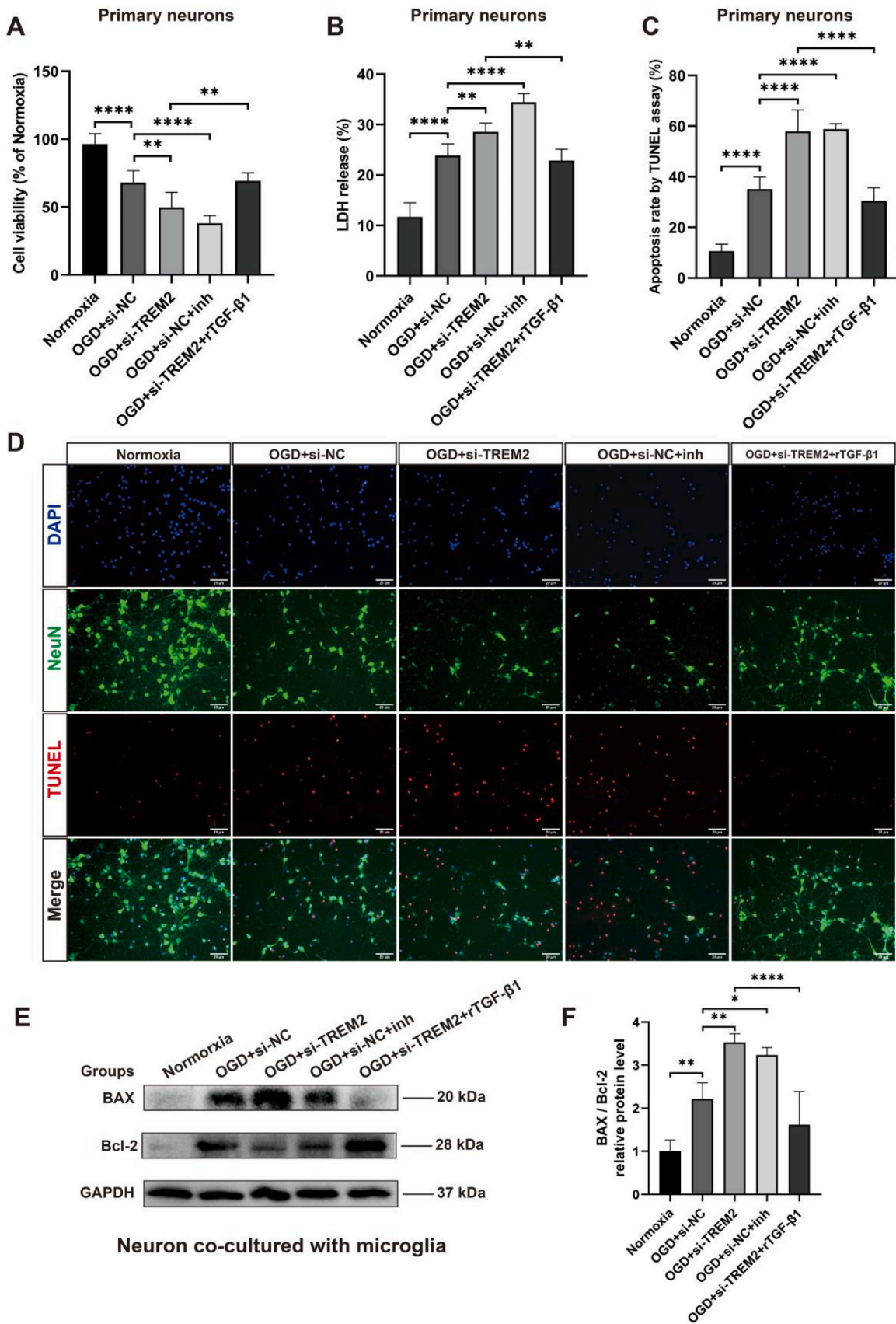
(caption on next page)

Fig. 5. TREM2 reduces neuronal cell death by upregulating TGF-β1 expression in microglia under conditions of hypoxia. A Cell viability was analyzed in primary neurons co-cultured with different microglia. The co-culture system was exposed to 4 h of OGD followed by 48 h of RO using the MTT assay in the five groups: group 1, neurons-microglia co-culture system under normoxia condition; group 2, neurons and negative control siRNA treated microglia co-culture with OGD/RO; group 3, neurons and siRNA-TREM2 treated co-culture with OGD/RO; group 4, neurons-microglia co-culture plus TGF-β1 receptor inhibitor treatment with OGD/RO; group 5, neurons and siRNA-TREM2 treated microglia co-culture plus recombinant TGF-β1 treatment with OGD/RO (n = 5). Neurons incubated under normoxic conditions were defined as 100% cell survival. B OGD-induced neuronal cell toxicity was further assessed by the lactate dehydrogenase (LDH) release assay in the aforementioned 5 groups (n = 5). C Quantitative analysis of apoptotic cell rate in primary neuron by TUNEL assay in the aforementioned 5 groups (n = 5). D Immunofluorescence staining of neuron (NeuN, green) and apoptotic cells (TUNEL, red) in neuron in the aforementioned 5 groups. E-F Quantitative analysis of anti-apoptotic protein Bcl-2 and pro-apoptotic protein BAX expression in primary neurons using Western blot analysis normalized with the housekeeping protein GAPDH in the same five groups (n = 3). Statistical tests: Data are expressed as mean ± SD, NS: no significance, *p < 0.05, * *p < 0.01, * **p < 0.001, and * ** *p < 0.0001. Scale bars, 20 μm (D). Abbreviation: OGD, oxygen-glucose deprivation; si-TREM2, TREM2 siRNA; inh, TGF-β1 receptor inhibitor; rTGF-β1, recombinant TGF-β1; MTT, thiazolyl blue tetrazolium bromide; LDH, lactate dehydrogenase; Bcl-2, B-cell lymphoma 2; BAX, Bcl-2-associated X protein.

3.8. TREM2 regulates cholesterol levels affecting M2 microglia polarization and post-stroke neurological recovery of mice

In light of the above in vitro data on TREM2 regulation of cholesterol levels and phenotypic polarization in microglia, we further verified whether or not TREM2 exerts similar effects under in vivo stroke conditions. Upon induction of stroke, only CE were significantly increased, whereas knockdown of TREM2 significant increased levels of TC, FC and CE. rTGF-β1 treatment significantly reduced the si-TREM2-induced CE upregulation, whereas FC was not significantly altered (Fig. 8A-C). Using flow cytometry analysis, the number of CD206 + microglia of the M2 phenotype was significantly decreased due to TREM2 knockdown (Fig. 8D-E). The gating strategy as well as additional FACS density plots are shown in Supplementary Fig. S7A-E. Assessing neurological recovery on days 5 and 7 post-stroke, si-TREM2 knockdown caused animals to perform significantly worse in the rotarod test, balance beam test, tightrope test, and corner turn test when compared to the MCAO-si-NC control and the si-TREM2 +rTGF-β1 treatment groups (Fig. 8F-I). These results are in favor of TREM2 knockdown significantly exacerbating motor coordination deficits in post-stroke mice.

4. Discussion

Neuroinflammation is a critical marker for secondary cell injury during the process of ischemic stroke [50,51]. Following the latter, the disruption of the blood-brain barrier along with neuronal cell death are accompanied by the activation of microglia [52–54]. Regulation of inflammation is one of the vital functions of microglia, which are generally divided into resting M0 microglia, pro-inflammatory M1 microglia, and anti-inflammatory M2 microglia [55–58]. Recent studies have identified a possible involvement of lipid metabolism in regulating microglia function [59,60], where TREM2 as a transmembrane protein responsible for lipid transport, has shown potential for a microglia-targeted therapy [10,12]. In the current study, knockdown of TREM2 led to a shift in microglia towards a pro-inflammatory M1 phenotype and a reduction in TGF-β1 levels in the ischemic stroke model. Our results indicated that upregulation of TREM2 in microglia could mitigate post-ischemic neuroinflammation and neuronal apoptosis, at least in part, through the TGF-β1/Smad2/3 signaling pathway and cholesterol synthesis.

Interestingly, TREM2-mediated microglial activation exhibits double-edged effects due to the different roles of activated microglia in different disease models [61]. Recent studies have shown that TREM2 with its ligands, DAP12 and ApoE, are the major pathways that shift microglia from a homeostatic state to a neurological disease-associated state [19,62,63]. TREM2 and its ligands are risk factors for neurodegenerative diseases [64,65], and activated microglia proliferate in the substantia nigra of brains and produce neurotoxic molecules, leading to the gradual degeneration of dopaminergic neurons in a non-cell-autonomous manner, and are therefore considered deleterious in pathological progress [66]. However, Jay et al. concluded that TREM2 deficiency leads to a reduction in inflammatory myeloid cell infiltration and ameliorates AD pathology in the early stages [67], while

exacerbating AD pathology in the late stages [68]. In stroke studies, the increase in the amount of microglia after ischemia was inhibited in TREM2 KO mice, and the proliferation and phagocytic activity of microglia were diminished, ultimately leading to deterioration in the neural scores of the mice [69,70]. Similarly, in our study, we also observed a time-dependent elevation of TREM2 expression in microglia exposed to hypoxia. This increase in TREM2 expression coincided with the upregulation of TGF-β1, microglial phagocytosis and polarization, while knockdown of TREM2 leads to severe neural damage. Hence, TREM2 exhibits a neuroprotective role in post-stroke injury.

Mounting evidence indicated that activated microglia release pro-/ anti-inflammatory cytokines, and play both a detrimental and protective role in post-ischemic damage [55,71]. However, whether TREM2 acts as a pro- or anti-inflammatory mediator in microglia remains unclear. One of the reasons for this controversy may be related to the different ligands mediated by TREM2 in acute or chronic inflammation. DAP12, one of the important ligands of TREM2, is the dominant switch that shifts microglia from a homeostatic state to a disease-associated state [62,72]. It increases the production of Aβ plaques and the spread of Tau proteins, accelerating brain pathology and behavioral deficits, and ultimately increasing the risk of many neurodegenerative diseases [72–75]. On the other hand, in a neurodegenerative diseases study, TREM2 restored microglia homeostasis by TREM2-APOE mediated pathways, which may be achieved by regulating major transcription factors homologous to microglia, including TGF-β [19]. TREM2 synergizes with its ligand APOE to bind to apoptotic neurons and increase TREM2-mediated phagocytosis [76]. In contrast, TREM2 deficiency may lock microglia in a homeostatic state and block essential microglia defenses during disease progression [77]. In our study, we also confirmed that the knockdown of TREM2 inhibited TGF-β1 and its downstream signaling, resulting in impaired microglial phagocytosis and failure of cellular debris clearance.

TREM2 has been shown to effectively influence diverse downstream pathways and molecules, including PI3K/Akt and TLR4/NF-κB signaling pathways, to regulate the expression of pro-inflammatory cytokines in microglia [78,79]. It promotes phagocytosis of apoptotic neurons and inhibits the expression of pro-inflammatory molecules such as TNF-α [80,81]. In the current study, knockdown of TREM2 expression in microglia followed by the downregulation of the TGF-β1/Smad2/3 signaling pathway, significantly reduced anti-inflammatory cytokine TGF-β1, further causing a notable decrease in M2 microglia, ultimately led to a loss of the neuroprotective effects exerted by microglia. This TREM2-modulated microglial phenotypic alteration was also validated in another study on LPS-induced neuroinflammation, that upregulation of TREM2 could contribute to the M2 anti-inflammatory microglia phenotype [79]. Moreover, in line with our findings, growing evidence has indicated that TREM2 can participate in the modulation of microglial polarization towards the M2 anti-inflammatory phenotype via various signaling pathways including TLR4-mediated pathways, JAK-/STAT pathway, and PI3K/Akt pathway [82–86]. However, the concept of "disease-associated microglia" (DAM) has recently emerged [19,87]. This high expression of TREM2 in "neurodegenerative phenotype microglia" in chronic neuroinflammatory diseases, at least in mouse
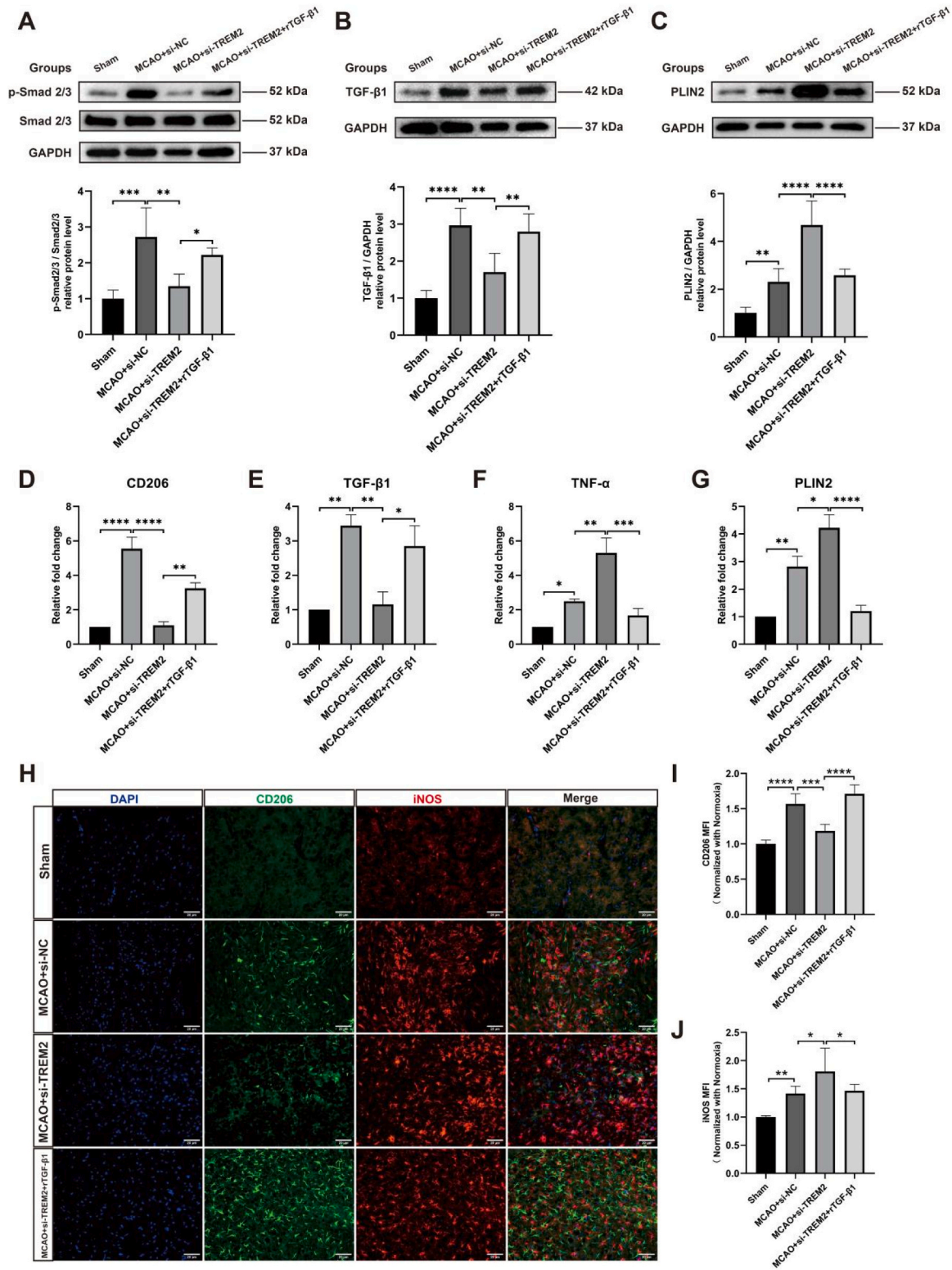
Fig. 6. TREM2 regulates post-stroke microglial polarization and inflammation in mice via the Smad2/3/TGF-β1 pathway. A-C Quantitative analysis of p-Smad2/3, Smad2/3 (A), TGF-β1 (B), and PLIN2 (C) expression in 4 groups (group 1, sham mice; group 2, MCAO mice treated with the negative control siRNA; group 3, MCAO mice treated with TREM2 siRNA; group 4, MCAO mice treated with TREM2 siRNA plus recombinant TGF-β1 treatment) by Western blot analysis of the ischemic hemisphere. Western blot was normalized with the housekeeping protein GAPDH (n = 3). D-G Quantitative analysis of CD206 (D), TGF-β1 (E), TNF-α (F), and PLIN2 (G) mRNA expression in the same four groups using quantitative real-time polymerase chain reaction (qRT-PCR) normalized with the housekeeping gene β-actin (n = 5). H Immunofluorescence staining of CD206 (green) and iNOS (red) in MCAO mice in the aforementioned 4 groups. I Quantitative analysis of the mean fluorescence intensity (MFI) of CD206 in the aforementioned 4 groups (n = 5). J Quantitative analysis of the mean fluorescence intensity (MFI) of CD68 in the aforementioned 4 groups (n = 5). Statistical tests: Data are expressed as mean ± SD, NS: no significance, *p < 0.05, * *p < 0.01, * **p < 0.001, * ** *p < 0.0001. Abbreviations: MCAO, middle cerebral artery occlusion; MFI, mean fluorescence intensity; TGF-β1, Transforming growth factor beta 1; PLIN2, Perilipin 2; TNF-α, Tumor necrosis factor alpha; iNOS, Nitric oxide synthase; si-TREM2, TREM2 siRNA; si-NC, Negative control siRNA; rTGF-β1, recombinant TGF-β1.
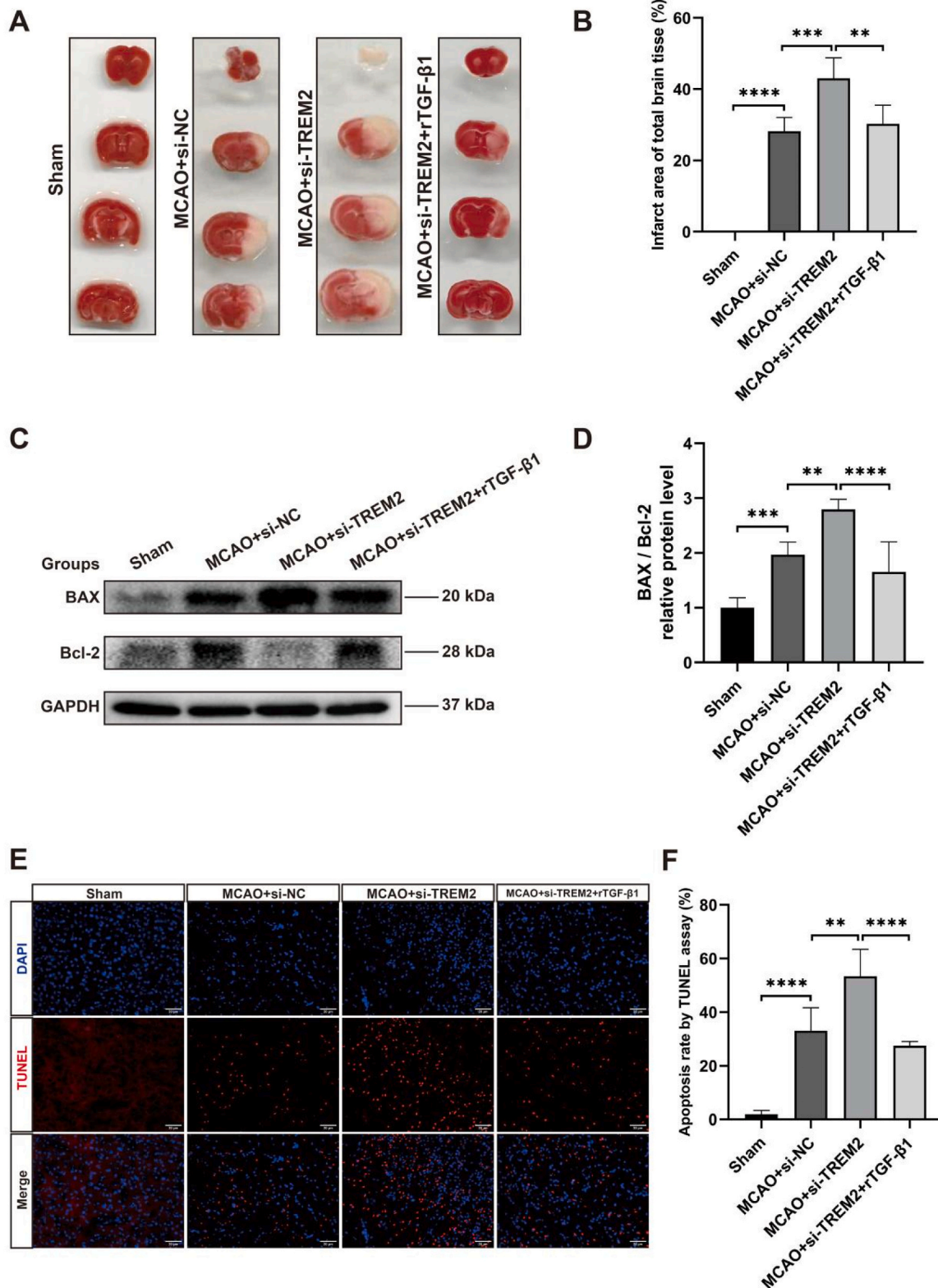
Fig. 7. TREM2 reduces post-stroke brain injury in mice. A-B 2,3,5-Triphenyltetrazolium chloride staining (TTC) image of brain infarction after 60 min MCAO (A). The white areas indicate the infarction sizes of the aforementioned 4 groups (B). C-D Quantitative analysis of anti-apoptotic protein Bcl-2 and pro-apoptotic protein BAX expression in the ischemic hemisphere of mice using Western blot analysis normalized with the housekeeping protein GAPDH in the aforementioned 4 groups (n = 3). E Immunofluorescence staining of apoptotic cell rate by TUNEL staining (red) in the 4 groups at post-ischemia day 7 in the aforementioned 4 groups. F Quantitative analysis of the apoptotic cell rate by TUNEL assay in the aforementioned 4 groups (n = 5). Statistical tests: Data are expressed as mean ± SD, NS: no significance, *p < 0.05, * *p < 0.01, * **p < 0.001, and * ** *p < 0.0001. Scale bars, 20 μm (E). Abbreviation: MCAO, middle cerebral artery occlusion; TTC, 2,3,5-Triphenyltetrazolium chloride staining; si-TREM2, TREM2 siRNA; si-NC, Negative control siRNA; rTGF-β1, recombinant TGF-β1; Bcl-2, B-cell lymphoma 2; BAX, Bcl-2-associated X protein.
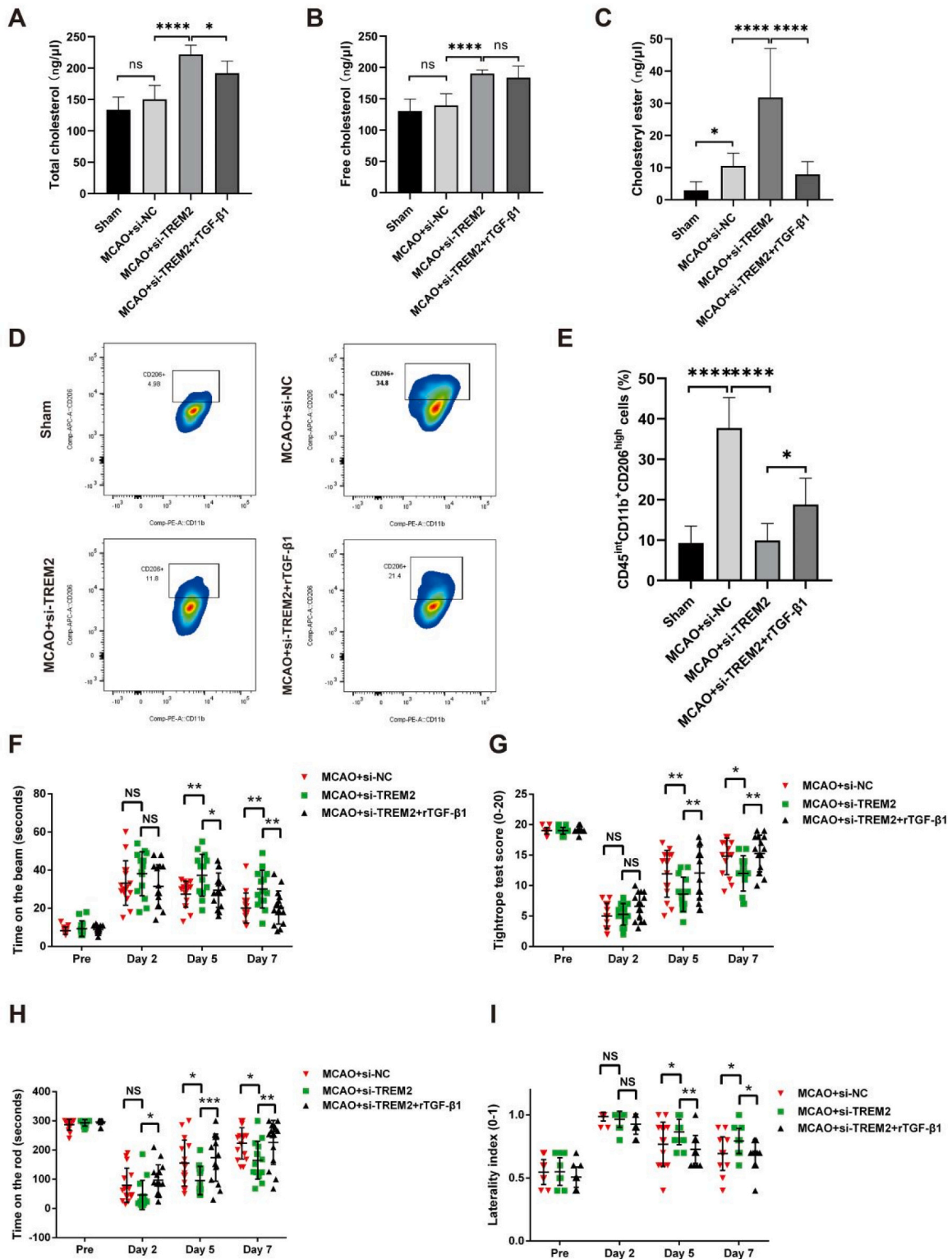
Fig. 8. TREM2 regulates cholesterol levels affecting M2 microglia polarization and post-stroke neurological recovery of mice. A-C Quantification of the level of total cholesterol (A), free cholesterol (B), and cholesteryl ester (C) in the ischemic hemisphere of mice in the aforementioned 4 groups (n = 5). D Density plots of fluorescence-activated cell sorting analysis (FACS) showed the numbers of M2-like microglia (CD45intCD11b+CD206 +) in the MCAO mice. E Quantitative analysis of CD45intCD11b+CD206 + microglia in the aforementioned 4 groups by flow cytometry (n = 5). F-I Silence of TREM2 aggravates post-ischemic motor coordination impairment via the TGF-β/Smad2/3 signaling pathway. Motor coordination was evaluated using the balance beam test (F), tightrope test (G), rotarod test (H), and corner turn test (I) 1 day before stroke (pre) as well as 2, 5 and 7 days after stroke. All animals were accordingly trained before the induction of stroke in order to ensure proper test performance (n = 15). Statistical tests: Data are expressed as mean ± SD, NS: no significance, *p < 0.05, * *p < 0.01, * **p < 0.001, and * ** *p < 0.0001. Abbreviation: MCAO, middle cerebral artery occlusion; FACS, fluorescence-activated cell sorting analysis; si-TREM2, TREM2 siRNA; si-NC, Negative control siRNA; rTGF-β1, recombinant TGF-β1.

models of AD and ALS, has been shown to be a major inducer of this deleterious phenotype [19,87]. Although the role of TREM2 in the phenotypic regulation of microglia is still controversial, at least in acute ischemic injury research, anti-inflammatory actions of resident microglia are, in part, mediated by TREM2, which is critically involved in anti-inflammation, anti-apoptosis and immunomodulation after ischemia [49,88].

Dysregulation of lipid metabolism is also a critical factor in the progression of microglia-mediated inflammation [89,90]. Lipid synthesis and cholesterol esterification are important for LD formation, and both lipid aggregation and LD formation are important hallmarks of microglia senescence and inflammation [91]. It has been shown that TREM2 can greatly reduce a variety of lipids, including CE and TAG, DAG, alleviate the lipid burden, and regulate the transition of physiological microglia to pathological DAM [92]. Previous studies demonstrated that TREM2 regulates lipid metabolism in the CNS including cholesterol, myelin, and phospholipids [15,92,93]. TREM2 knockdown of microglia exhibited severe CE storage impairment, similar to foamy microglia or macrophages in chronic neuroinflammatory diseases [15, 92]. This disruption of the dynamic balance of lipid metabolism resulted in the accumulation of a variety of lipids, including cholesterol, which produces peroxidation-induced pro-inflammatory toxic [94]. In our study, LD accumulation and cholesterol over-synthesis after ischemia may promote neuronal death and inflammatory responses. The mRNA levels of LMRGs were significantly upregulated after ischemia, resulting in increased lipid synthesis and decreased cholesterol clearance and lipid hydrolysis, and rTGF-β1 did not alter LMRG mRNA levels. Furthermore, TREM2 knockdown resulted in upregulation of CE, FC, and TC in the mouse brain accompanied by severe neurological deficits, whereas TGF-β1 receptor inhibitors did not affect cholesterol levels, and rTGF-β1, in turn, reduced cholesterol levels after ischemia. The possible mechanism is that, albeit microglial cholesterol metabolism is independent of the TGF-β/Smad2/3 pathway, the anti-inflammatory factor reduces the expression of various key factors of lipid synthesis [95]. Furthermore, the knockdown of TREM2 impaired cholesterol clearance in microglia, and phagocytized cholesterol converted to CE, finally forming LD-rich microglia. Thus, TREM2 may play a vital role in both the direct regulation of inflammation through the TGF-β1/Smad2/3 pathway and via regulating lipid metabolic processes followed by the impact on the microglial phenotype [84]. The cholesterol burden caused by this process might also contribute to impaired phagocytosis in microglia. Our results validate the recent findings that TREM2 may mediate CE clearance and phagocytosis in microglia by regulating lipid metabolism [15,96], suggesting a promising link between TREM2 and lipid metabolism.

Despite the conflicting findings on the beneficial or detrimental effects of TREM2, emerging evidence from a combination of preclinical and clinical studies strongly indicates that a novel soluble form of TREM2 (sTREM2) exhibits a protective role against AD pathology [97]. However, the precise mechanisms mediating sTREM2 function remain largely unknown. In addition, in a study of tetravalent TREM2 agonistic antibodies in AD, TREM2 activation was increased 100-fold by modification of the TREM2 into a tetravalent variable structural domain immunoglobulin (TVD-Ig) [98]. TREM2 activation enhanced phagocytosis of lipid complexes by microglial and reduced endogenous tau hyperphosphorylation, improving cognitive function, albeit antibody-based treatment remained low potency and difficulty crossing the blood-brain barrier [98,99]. Another study of anti-human TREM2 have revealed that TREM2 deficiency impairs key substrates of phagocytosis including APOE, inhibits SDF-1α/CXCR4-mediated chemotaxis, and ultimately leads to impaired responses to β-amyloid plaques [34]. Likewise, upregulation of TREM2 improved cognitive function by enhancing microglia phagocytosis and inhibiting pro-inflammatory responses, including Aβ deposition, neuroinflammation and synaptic loss [100]. Additionally, a potential function of TREM2 by modulating the macrophage anti-mycobacterial response was identified that human

TREM2 binds specifically to the pathogenic mycobacterium tuberculosis (MT), promotes macrophage uptake of MT, and is responsible for the blockade of TNF-α, IL-1β, and the enhancement of interferon-β (IFN-β) and IL-10 production [101]. Therefore, antibody-mediated or pharmacologic targeting of TREM2 may be a promising new strategy for the treatment of multiple inflammatory diseases.

In conclusion, our present work demonstrates that TREM2 plays an important role in ischemic brain injury. TREM2 attenuates post-ischemic injury by upregulating the TGF-β/Smad2/3 signaling pathway, contributing to the M2-type anti-inflammatory polarization of microglia, reducing cholesterol loading, and maintaining microglial phagocytosis. Our work highlights the therapeutic potential of TREM2 in ischemic stroke conditions, making TREM2 an attractive new clinical target for the treatment of ischemic stroke and other inflammation-related diseases. However, the specific mechanism of TREM2-associated signaling modulation must be further investigated before a clinical translation is in order.

Ethics statement

This article does not contain any studies with human participants. All animal experiments were performed with governmental approval according to the NIH guidelines for the care and use of laboratory animals. Both the STAIR criteria and the ARRIVE guidelines have been followed.

Funding statement

CRediT author contribution statement

Wei Wei: Conceptualization, Methodology, Formal analysis, Software, Writing – original draft. **Lin Zhang**: Conceptualization, Programming, Data curation, Writing- original draft. **Wenqiang Xin**: Formal analysis, Visualization, Investigation, Writing – original draft. **Yongli Pan**: Methodology, Formal analysis, Software, Programming. **Lars Tatenhorst**: Writing – original draft, Software, Validation. **Zhongnan Hao**: Writing – original draft, Software, Methodology. **Stefan T Gerner**: Writing – review & editing. **Sabine Huber**: Resources, Data curation. **Martin Juenemann**: Writing – original draft, Software. **Marius Butz**: Visualization. **Hagen B Huttner**: Supervision, Project administration. **Mathias Bähr**: Supervision, Project administration, Funding acquisition. **Dirk Fitzner**: Writing – original draft, Supervision, Project administration, Funding acquisition. **Feng Jia**: Conceptualization, Supervision, Project administration, Funding acquisition. **Thorsten R Doeppner**: Conceptualization, Writing – original draft, Supervision, Project administration, Funding acquisition.

Declaration of Competing Interest

The authors declare that they have no known competing financial interests or personal relationships that could have appeared to influence the work reported in this paper.

Data Availability

Data will be made available on request. All data generated or analyzed during this study are included in this published article and its supplementary information files.

Acknowledgment

We thank Irina Graf for excellent technical assistance.

Author contribution statement

WW, LZ, WQX, YLP, LT, STG, SH and MB performed the experiments. WW, LZ, FJ, DF, and TRD designed the study. TRD, DF, FJ and HBH provided financial support. WW, LZ, WQX, YLP, LT, ZH, STG, SH, MJ, MB, HBH, MB, DF, FJ, and TRD wrote the manuscript.

Appendix A. Supporting information

Supplementary data associated with this article can be found in the online version at doi:10.1016/j.biopha.2023.115962.

References

[1] M. Kanazawa, I. Ninomiya, M. Hatakeyama, T. Takahashi, T. Shimohata, Microglia and monocytes/macrophages polarization reveal novel therapeutic mechanism against stroke, Int J. Mol. Sci. 18 (10) (2017).

[2] C. Qin, L.Q. Zhou, X.T. Ma, Z.W. Hu, S. Yang, M. Chen, D.B. Bosco, L.J. Wu, D. S. Tian, Dual functions of microglia in ischemic stroke, Neurosci. Bull. 35 (5) (2019) 921–933.

[3] D. Nayak, T.L. Roth, D.B. McGavern, Microglia development and function, Annu. Rev. Immunol. 32 (2014) 367–402.

[4] X. Hu, P. Li, Y. Guo, H. Wang, R.K. Leak, S. Chen, Y. Gao, J.J.S. Chen, Microglia/macrophage polarization dynamics reveal novel mechanism of injury expansion after focal cerebral ischemia 43 (11) (2012) 3063–3070.

[5] J. Jia, L. Yang, Y. Chen, L. Zheng, Y. Chen, Y. Xu, M. Zhang, The role of microglial phagocytosis in ischemic stroke, Front Immunol. 12 (2021), 790201.

[6] C. Herzog, L. Pons Garcia, M. Keatinge, D. Greenald, C. Moritz, F. Peri, L. Herrgen, Rapid clearance of cellular debris by microglia limits secondary neuronal cell death after brain injury in vivo, Development 146 (9) (2019).

[7] H. Wang, X. Li, Q. Wang, J. Ma, X. Gao, M. Wang, TREM2, microglial and ischemic stroke, J. Neuroimmunol. 381 (2023), 578108.

[8] T.K. Ulland, M. Colonna, TREM2 - a key player in microglial biology and Alzheimer disease, Nat. Rev. Neurol. 14 (11) (2018) 667–675.

[9] P. Gervois, I. Lambrichts, The emerging role of triggering receptor expressed on myeloid cells 2 as a target for immunomodulation in ischemic stroke, Front Immunol. 10 (2019) 1668.

[10] R. Wu, X. Li, P. Xu, L. Huang, J. Cheng, X. Huang, J. Jiang, L.J. Wu, Y. Tang, TREM2 protects against cerebral ischemia/reperfusion injury, Mol. brain 10 (1) (2017) 20.

[11] K. Kurisu, Z. Zheng, J.Y. Kim, J. Shi, A. Kanoke, J. Liu, C.L. Hsieh, M.A. Yenari, Triggering receptor expressed on myeloid cells-2 expression in the brain is required for maximal phagocytic activity and improved neurological outcomes following experimental stroke, J. Cereb. Blood Flow. Metab. 39 (10) (2019) 1906–1918.

[12] Q. Zhai, F. Li, X. Chen, J. Jia, S. Sun, D. Zhou, L. Ma, T. Jiang, F. Bai, L. Xiong, Q. Wang, Triggering receptor expressed on myeloid cells 2, a novel regulator of immunocyte phenotypes, confers neuroprotection by relieving neuroinflammation, Anesthesiology 127 (1) (2017) 98–110.

[13] S. Chen, J. Peng, P. Sherchan, Y. Ma, S. Xiang, F. Yan, H. Zhao, Y. Jiang, N. Wang, J.H. Zhang, H. Zhang, TREM2 activation attenuates neuroinflammation and neuronal apoptosis via PI3K/Akt pathway after intracerebral hemorrhage in mice, J. Neuroinflamm. 17 (1) (2020), 168.

[14] S. Liu, X. Cao, Z. Wu, S. Deng, H. Fu, Y. Wang, F. Liu, TREM2 improves neurological dysfunction and attenuates neuroinflammation, TLR signaling and neuronal apoptosis in the acute phase of intracerebral hemorrhage, Front Aging Neurosci. 14 (2022), 967825.

[15] A.A. Nugent, K. Lin, B. van Lengerich, S. Lianoglou, L. Przybyla, S.S. Davis, C. Llapashtica, J. Wang, D.J. Kim, D. Xia, A. Lucas, S. Baskaran, P.C.G. Haddick, M. Lenser, T.K. Earr, J. Shi, J.C. Dugas, B.J. Andreone, T. Logan, H.O. Solanoy, H. Chen, A. Srivastava, S.B. Poda, P.E. Sanchez, R.J. Watts, T. Sandmann, G. Astarita, J.W. Lewcock, K.M. Monroe, G. Di Paolo, TREM2 regulates microglial cholesterol metabolism upon chronic phagocytic challenge, Neuron 105 (5) (2020), 837-854.e9.

[16] X. Guo, B. Li, C. Wen, F. Zhang, X. Xiang, L. Nie, J. Chen, L. Mao, TREM2 promotes cholesterol uptake and foam cell formation in atherosclerosis, Cell. Mol. life Sci.: CMLS 80 (5) (2023), 137.

[17] F. Cignarella, F. Filipello, B. Bollman, C. Cantoni, A. Locca, R. Mikesell, M. Manis, A. Ibrahim, L. Deng, B.A. Benitez, C. Cruchaga, D. Licastro, K. Mihindukulasuriya, O. Harari, M. Buckland, D.M. Holtzman, A. Rosenthal, T. Schwabe, I. Tassi, L. Piccio, TREM2 activation on microglia promotes myelin debris clearance and remyelination in a model of multiple sclerosis, Acta Neuropathol. 140 (4) (2020) 513–534.

[18] X. Xiang, G. Werner, B. Bohrmann, A. Liesz, F. Mazaheri, A. Capell, R. Feederle, I. Knuesel, G. Kleinberger, C. Haass, TREM2 deficiency reduces the efficacy of immunotherapeutic amyloid clearance, EMBO Mol. Med. 8 (9) (2016) 992–1004.

[19] S. Krasemann, C. Madore, R. Cialic, C. Baufeld, N. Calcagno, R. El Fatimy, L. Beckers, E. O'Loughlin, Y. Xu, Z. Fanek, D.J. Greco, S.T. Smith, G. Tweet, Z. Humulock, T. Zrzavy, P. Conde-Sanroman, M. Gacias, Z. Weng, H. Chen, E. Tjon, F. Mazaheri, K. Hartmann, A. Madi, J.D. Ulrich, M. Glatzel, A. Worthmann, J. Heeren, B. Budnik, C. Lemere, T. Ikezu, F.L. Heppner, V. Litvak, D.M. Holtzman, H. Lassmann, H.L. Weiner, J. Ochando, C. Haass, O. Butovsky, The TREM2-APOE Pathway drives the transcriptional phenotype of dysfunctional microglia in neurodegenerative diseases, Immunity 47 (3) (2017) 566–581.e9.

[20] J. Marschallinger, T. Iram, M. Zardeneta, S.E. Lee, B. Lehallier, M.S. Haney, J. V. Pluvinage, V. Mathur, O. Hahn, D.W.J.Nn Morgens, Lipid-droplet-accumulating microglia represent a dysfunctional and proinflammatory state in the aging brain 23 (2) (2020) 194–208.

[21] C. Claes, E.P. Danhash, J. Hasselmann, J.P. Chadarevian, S.K. Shabestari, W. E. England, T.E. Lim, J.L.S. Hidalgo, R.C. Spitale, H. Davtyan, M. Blurton-Jones, Plaque-associated human microglia accumulate lipid droplets in a chimeric model of Alzheimer's disease, Mol. Neurodegener. 16 (1) (2021), 50.

[22] R. Afridi, W.H. Lee, K. Suk, Microglia gone awry: linking immunometabolism to neurodegeneration, Front Cell Neurosci. 14 (2020), 246.

[23] X.W. Pang, Y.H. Chu, L.Q. Zhou, M. Chen, Y.F. You, Y. Tang, S. Yang, H. Zhang, J. Xiao, G. Deng, W. Wang, K. Shang, C. Qin, D.S. Tian, Trem2 deficiency attenuates microglial phagocytosis and autophagic-lysosomal activation in white matter hypoperfusion, J. Neurochem. 167 (4) (2023) 489–504.

[24] G. Gouna, C. Klose, M. Bosch-Queralt, L. Liu, O. Gokce, M. Schifferer, L. Cantuti-Castelvetri, M. Simons, TREM2-dependent lipid droplet biogenesis in phagocytes is required for remyelination, J. Exp. Med 218 (10) (2021).

[25] C. Cantoni, B. Bollman, D. Licastro, M. Xie, R. Mikesell, R. Schmidt, C.M. Yuede, D. Galimberti, G. Olivecrona, R.S. Klein, A.H. Cross, K. Otero, L. Piccio, TREM2 regulates microglial cell activation in response to demyelination in vivo, Acta Neuropathol. 129 (3) (2015) 429–447.

[26] A. Islam, M.E. Choudhury, Y. Kigami, R. Utsunomiya, S. Matsumoto, H. Watanabe, Y. Kumon, T. Kunieda, H. Yano, J. Tanaka, Sustained anti-inflammatory effects of TGF-β1 on microglia/macrophages, Biochim Biophys. Acta Mol. Basis Dis. 1864 (3) (2018) 721–734.

[27] B. Spittau, N. Dokalis, M. Prinz, The Role of TGFβ Signaling in Microglia Maturation and Activation, Trends Immunol. 41 (9) (2020) 836–848.

[28] X. Yao, P. Li, Y. Deng, Y. Yang, H. Luo, B. He, Role of p53 in promoting BMP9-induced osteogenic differentiation of mesenchymal stem cells through TGF-β1, Exp. Ther. Med 25 (6) (2023), 248.

[29] T.L. Kieu, L. Pierre, V. Derangère, S. Perrey, C. Truntzer, A. Jalil, S. Causse, E. Groetz, A. Dumont, L. Guyard, L. Arnould, J.P. de Barros, L. Apetoh, C. Rébé, E. Limagne, T. Jourdan, L. Demizieux, D. Masson, C. Thomas, F. Ghiringhelli, M. Rialland, Downregulation of Elovl5 promotes breast cancer metastasis through a lipid-droplet accumulation-mediated induction of TGF-β receptors, Cell Death Dis. 13 (9) (2022), 758.

[30] Z. Zhang, Y. Meng, F. Gao, Y. Xiao, Y. Zheng, H.Q. Wang, Y. Gao, H. Jiang, B. Yuan, J.B. Zhang, TGF-β1-mediated fdncr1 regulates porcine preadipocyte differentiation via the TGF-β signaling pathway, Anim.: Open Access J. MDPI 10 (8) (2020).

[31] D. Bose, S. Banerjee, N. Chatterjee, S. Das, M. Saha, K.D. Saha, Inhibition of TGF-β induced lipid droplets switches M2 macrophages to M1 phenotype, Toxicol. Vitr.: Int. J. Publ. Assoc. BIBRA 58 (2019) 207–214.

[32] R.A. Taylor, C.F. Chang, B.A. Goods, M.D. Hammond, B.Mac Grory, Y. Ai, A. F. Steinschneider, S.C. Renfroe, M.H. Askenase, L.D. McCullough, S.E. Kasner, M. T. Mullen, D.A. Hafler, J.C. Love, L.H. Sansing, TGF-β1 modulates microglial phenotype and promotes recovery after intracerebral hemorrhage, J. Clin. Invest 127 (1) (2017) 280–292.

[33] J. Avila, The role of TGF-β1 in promoting microglial Aβ phagocytosis, Neuroscience 438 (2020) 215–216.

[34] A. McQuade, Y.J. Kang, J. Hasselmann, A. Jairaman, A. Sotelo, M. Coburn, S. K. Shabestari, J.P. Chadarevian, G. Fote, C.H. Tu, E. Danhash, J. Silva, E. Martinez, C. Cotman, G.A. Prieto, L.M. Thompson, J.S. Steffan, I. Smith, H. Davtyan, M. Cahalan, H. Cho, M. Blurton-Jones, Gene expression and functional deficits underlie TREM2-knockout microglia responses in human models of Alzheimer's disease, Nat. Commun. 11 (1) (2020), 5370.

[35] X. Zhuang, Y. Yu, Y. Jiang, S. Zhao, Y. Wang, L. Su, K. Xie, Y. Yu, Y. Lu, G. Lv, Molecular hydrogen attenuates sepsis-induced neuroinflammation through regulation of microglia polarization through an mTOR-autophagy-dependent pathway, Int. Immunopharmacol. 81 (2020), 106287.

[36] P. Li, T. Shen, X. Luo, J. Yang, Z. Luo, Y. Tan, G. He, Z. Wang, X. Yu, Y. Wang, X. Yang, Modulation of microglial phenotypes by dexmedetomidine through TREM2 reduces neuroinflammation in heatstroke, Sci. Rep. 11 (1) (2021), 13345.

[37] K. Sugimoto, R. Nishioka, A. Ikeda, A. Mise, H. Takahashi, H. Yano, Y. Kumon, T. Ohnishi, J. Tanaka, Activated microglia in a rat stroke model express NG2 proteoglycan in peri-infarct tissue through the involvement of TGF-β1, Glia 62 (2) (2014) 185–198.

[38] J. Hou, Y. Chen, G. Grajales-Reyes, M. Colonna, TREM2 dependent and independent functions of microglia in Alzheimer's disease, Mol. Neurodegener. 17 (1) (2022), 84.

[39] F. Filipello, R. Morini, I. Corradini, V. Zerbi, A. Canzi, B. Michalski, M. Erreni, M. Markicevic, C. Starvaggi-Cucuzza, K. Otero, L. Piccio, F. Cignarella, F. Perrucci, M. Tamborini, M. Genua, L. Rajendran, E. Menna, S. Vetrano, M. Fahnestock, R.C. Paolicelli, M. Matteoli, The microglial innate immune receptor TREM2 is required for synapse elimination and normal brain connectivity, Immunity 48 (5) (2018) 979–991.e8.

[40] H. Lian, E. Roy, H. Zheng, Protoc. Prim. Micro Cult. Prep. 6 (21) (2016) e1989-e1989.

[41] T. Fath, Y.D. Ke, P. Gunning, J. Götz, L.M. Ittner, Primary support cultures of hippocampal and substantia nigra neurons 4 (1) (2009) 78–85.

[42] S.D. Skaper, L. Facci, Central nervous system neuron-glia co-culture models and application to neuroprotective agents. Neurotrophic Factors, Springer, 2018, pp. 63–80.

[43] T.L. Riss, R.A. Moravec, A.L. Niles, S. Duellman, H.A. Benink, T.J. Worzella, L. Minor, Cell viability assays, Assay Guidance Manual (2016).

[44] T.R. Doeppner, J. Herz, A. Görgens, J. Schlechter, A.-K. Ludwig, S. Radtke, K. de Miroschedji, P.A. Horn, B. Giebel, D.M.J.Sctm Hermann, Extracell. vesicles Improv. Post.-Stroke neuroregeneration Prev. Post. Immunosuppr. 4 (10) (2015) 1131–1143.

[45] M. Balkaya, J.M. Kröber, A. Rex, M. Endres, Assessing post-stroke behavior in mouse models of focal ischemia, J. Cereb. Blood Flow. Metab. 33 (3) (2013) 330–338.

[46] Q. Guo, G. Wang, X. Liu, S. Namura, Effects of gemfibrozil on outcome after permanent middle cerebral artery occlusion in mice, Brain Res 1279 (2009) 121–130.

[47] T. Freret, V. Bouet, C. Leconte, S. Roussel, L. Chazalviel, D. Divoux, P. Schumann-Bard, M. Boulouard, Behavioral deficits after distal focal cerebral ischemia in mice: Usefulness of adhesive removal test, Behav. Neurosci. 123 (1) (2009) 224–230.

[48] W. Xin, Y. Pan, W. Wei, L. Tatenhorst, I. Graf, A. Popa-Wagner, S.T. Gerner, S. Huber, E. Kilic, D.M. Hermann, M. Bähr, H.B. Huttner, T.R. Doeppner, Preconditioned extracellular vesicles from hypoxic microglia reduce poststroke AQP4 depolarization, disturbed cerebrospinal fluid flow, astrogliosis, and neuroinflammation, Theranostics 13 (12) (2023) 4197–4216.

[49] L. Zhang, W. Wei, X. Ai, E. Kilic, D.M. Hermann, V. Venkataramani, M. Bähr, T. R. Doeppner, Extracellular vesicles from hypoxia-preconditioned microglia promote angiogenesis and repress apoptosis in stroke mice via the TGF-β/Smad2/3 pathway, Cell Death Dis. 12 (11) (2021), 1068.

[50] R.L. Jayaraj, S. Azimullah, R. Beiram, F.Y. Jalal, G.A.J.Jon Rosenberg, Neuroinflamm.: Friend foe ischemic Stroke 16 (1) (2019) 1–24.

[51] X.-Y. Xiong, L. Liu, Q.-W.J.Pin Yang, Funct. Mech. Micro /macrophages Neuroinflamm. neurogenesis Stroke 142 (2016) 23–44.

[52] D. Radak, N. Katsiki, I. Resanovic, A. Jovanovic, E. Sudar-Milovanovic, S. Zafirovic, S.A. Mousad, E.J.Cvp R Isenovic, Apoptosis acute brain ischemia ischemic Stroke 15 (2) (2017) 115–122.

[53] J. Anrather, C.J.N. Iadecola, Inflamm. Stroke.: Overv. 13 (4) (2016) 661–670.

[54] C. Xing, K. Arai, E.H. Lo, M. Hommel, Pathophysiologic cascades in ischemic stroke, Int. J. Stroke 7 (5) (2012) 378–385.

[55] W. Zhang, T. Tian, S.-X. Gong, W.-Q. Huang, Q.-Y. Zhou, A.-P. Wang, Y. Tian, Microglia-associated neuroinflammation is a potential therapeutic target for ischemic stroke 16 (1) (2021) 6.

[56] S. Yang, C. Qin, Z.-W. Hu, L.-Q. Zhou, H.-H. Yu, M. Chen, D.B. Bosco, W. Wang, L.-J. Wu, D. Tian, Micro reprogram Metab, Profiles phenotype Funct. Chang. Cent. Nerv. Syst. 152 (2021), 105290.

[57] C. Qin, L.-Q. Zhou, X.-T. Ma, Z.-W. Hu, S. Yang, M. Chen, D.B. Bosco, L.-J. Wu, D.-S. Tian, Dual functions of microglia in ischemic stroke 35 (5) (2019) 921–933.

[58] J.D. Cherry, J.A. Olschowka, M.K. O'Banion, Neuroinflamm. M2 Micro.: good, Bad., inflamed 11 (1) (2014) 1–15.

[59] A.A. Nugent, K. Lin, B. Van Lengerich, S. Lianoglou, L. Przybyla, S.S. Davis, C. Llapashtica, J. Wang, D. Xia, A.J.N. Lucas, TREM2 Regul. Micro Cholest. Metab. Chronic phagocytic Chall. 105 (5) (2020), 837-854. e9.

[60] S. Krasemann, C. Madore, R. Cialic, C. Baufeld, N. Calcagno, R. El Fatimy, L. Beckers, E. O'Loughlin, Y. Xu, Z.J.I. Fanek, TREM2-APOE Pathw. Drives Transcr. phenotype Dysfunct. Micro Neurodegener. Dis. 47 (3) (2017), 566-581. e9.

[61] H. Konishi, H. Kiyama, Microglial TREM2/DAP12 Signaling: A Double-Edged Sword in Neural, Dis., Front. Cell. Neurosci. 12 (2018) 206.

[62] Y. Zhou, M. Tada, Z. Cai, P.S. Andhey, A. Swain, K.R. Miller, S. Gilfillan, M. N. Artyomov, M. Takao, A. Kakita, M. Colonna, Human early-onset dementia caused by DAP12 deficiency reveals a unique signature of dysregulated microglia, Nat. Immunol. 24 (3) (2023) 545–557.

[63] C. Mecca, I. Giambanco, R. Donato, C. Arcuri, Microglia and aging: the role of the TREM2-DAP12 and CX3CL1-CX3CR1 Axes, Int. J. Mol. Sci. 19 (1) (2018).

[64] S. Rayaprolu, B. Mullen, M. Baker, T. Lynch, E. Finger, W.W. Seeley, K. J. Hatanpaa, A. Lomen-Hoerth, A. Kertesz, E.H. Bigio, C. Lippa, K.A. Josephs, D. S. Knopman, C.L. White, 3rd, R. Caselli, I.R. Mackenzie, B.L. Miller, M. Boczarska-Jedynak, G. Opala, A. Krygowska-Wajs, M. Barcikowska, S.G. Younkin, R. C. Petersen, N. Ertekin-Taner, R.J. Uitti, J.F. Meschia, K.B. Boylan, B.F. Boeve, N. R. Graff-Radford, Z.K. Wszolek, D.W. Dickson, R. Rademakers, O.A. Ross, TREM2 in neurodegeneration: evidence for association of the p.R47H variant with frontotemporal dementia and Parkinson's disease, Mol. Neurodegener. 8 (2013) 19.

[65] Y. Wang, M. Cella, K. Mallinson, J.D. Ulrich, K.L. Young, M.L. Robinette, S. Gilfillan, G.M. Krishnan, S. Sudhakar, B.H. Zinselmeyer, D.M. Holtzman, J. R. Cirrito, M. Colonna, TREM2 lipid sensing sustains the microglial response in an Alzheimer's disease model, Cell 160 (6) (2015) 1061–1071.

[66] X. Hu, D. Zhang, H. Pang, W.M. Caudle, Y. Li, H. Gao, Y. Liu, L. Qian, B. Wilson, D.A. Di Monte, S.F. Ali, J. Zhang, M.L. Block, J.S. Hong, Macrophage antigen complex-1 mediates reactive microgliosis and progressive dopaminergic neurodegeneration in the MPTP model of Parkinson's disease, J. Immunol. (Baltim., Md.: 1950) 181 (10) (2008) 7194–7204.

[67] T.R. Jay, C.M. Miller, P.J. Cheng, L.C. Graham, S. Bemiller, M.L. Broihier, G. Xu, D. Margevicius, J.C. Karlo, G.L. Sousa, A.C. Cotleur, O. Butovsky, L. Bekris, S. M. Staugaitis, J.B. Leverenz, S.W. Pimplikar, G.E. Landreth, G.R. Howell, R.

M. Ransohoff, B.T. Lamb, TREM2 deficiency eliminates TREM2+ inflammatory macrophages and ameliorates pathology in Alzheimer's disease mouse models, J. Exp. Med. 212 (3) (2015) 287–295.

[68] T.R. Jay, A.M. Hirsch, M.L. Broihier, C.M. Miller, L.E. Neilson, R.M. Ransohoff, B. T. Lamb, G.E. Landreth, Disease progression-dependent effects of TREM2 deficiency in a mouse model of Alzheimer's Disease, J. Neurosci.: Off. J. Soc. Neurosci. 37 (3) (2017) 637–647.

[69] M.W. Sieber, N. Jaenisch, M. Brehm, M. Guenther, B. Linnartz-Gerlach, H. Neumann, O.W. Witte, C. Frahm, Attenuated inflammatory response in triggering receptor expressed on myeloid cells 2 (TREM2) knock-out mice following stroke, PloS One 8 (1) (2013), e52982.

[70] M. Kawabori, R. Kacimi, T. Kauppinen, C. Calosing, J.Y. Kim, C.L. Hsieh, M. C. Nakamura, M.A. Yenari, Triggering receptor expressed on myeloid cells 2 (TREM2) deficiency attenuates phagocytic activities of microglia and exacerbates ischemic damage in experimental stroke, The, J. Neurosci.: Off. J. Soc. Neurosci. 35 (8) (2015) 3384–3396.

[71] A. Fernandes, L. Miller-Fleming, T.F. Pais, M. L. Sci., Micro InflamM.: Conspir., Controv. Or. Control? 71 (20) (2014) 3969–3985.

[72] S. Wang, R. Sudan, V. Peng, Y. Zhou, S. Du, C.M. Yuede, T. Lei, J. Hou, Z. Cai, M. Cella, K. Nguyen, P.L. Poliani, W.L. Beatty, Y. Chen, S. Cao, K. Lin, C. Rodrigues, A.H. Ellebedy, S. Gilfillan, G.D. Brown, D.M. Holtzman, S. Brioschi, M. Colonna, TREM2 drives microglia response to amyloid-β via SYK-dependent and -independent pathways, Cell 185 (22) (2022), 4153-4169.e19.

[73] A. Boza-Serrano, R. Ruiz, R. Sanchez-Varo, J. García-Revilla, Y. Yang, I. Jimenez-Ferrer, A. Paulus, M. Wennström, A. Vilalta, D. Allendorf, J.C. Davila, J. Stegmayr, S. Jiménez, M.A. Roca-Ceballos, V. Navarro-Garrido, M. Swanberg, C.L. Hsieh, L.M. Real, E. Englund, S. Linse, H. Leffler, U.J. Nilsson, G.C. Brown, A. Gutierrez, J. Vitorica, J.L. Venero, T. Deierborg, Galectin-3, a novel endogenous TREM2 ligand, detrimentally regulates inflammatory response in Alzheimer's disease, Acta Neuropathol. 138 (2) (2019) 251–273.

[74] T. Natunen, H. Martiskainen, M. Marttinen, S. Gabbouj, H. Koivisto, S. Kemppainen, S. Kaipainen, M. Takalo, H. Svobodová, L. Leppänen, B. Kemiläinen, S. Ryhänen, T. Kuulasmaa, E. Rahunen, S. Juutinen, P. Mäkinen, P. Miettinen, T. Rauramaa, J. Pihlajamäki, A. Haapasalo, V. Leinonen, H. Tanila, M. Hiltunen, Diabetic phenotype in mouse and humans reduces the number of microglia around β-amyloid plaques, Mol. Neurodegener. 15 (1) (2020), 66.

[75] X. Cui, J. Qiao, S. Liu, M. Wu, W. Gu, Mechanism of TREM2/DAP12 complex affecting β-amyloid plaque deposition in Alzheimer's disease modeled mice through mediating inflammatory response, Brain Res. Bull. 166 (2021) 21–28.

[76] Y. Atagi, C.C. Liu, M.M. Painter, X.F. Chen, C. Verbeeck, H. Zheng, X. Li, R. Rademakers, S.S. Kang, H. Xu, S. Younkin, P. Das, J.D. Fryer, G. Bu, Apolipoprotein E is a ligand for triggering receptor expressed on myeloid cells 2 (TREM2), J. Biol. Chem. 290 (43) (2015) 26043–26050.

[77] F. Mazaheri, N. Snaidero, G. Kleinberger, C. Madore, A. Daria, G. Werner, S. Krasemann, A. Capell, D. Trümbach, W. Wurst, B. Brunner, S. Bultmann, M. Tahirovic, M. Kerschensteiner, T. Misgeld, O. Butovsky, C. Haass, TREM2 deficiency impairs chemotaxis and microglial responses to neuronal injury, EMBO Rep. 18 (7) (2017) 1186–1198.

[78] Y. Wang, Y. Lin, L. Wang, H. Zhan, X. Luo, Y. Zeng, W. Wu, X. Zhang, F. Wang, TREM2 ameliorates neuroinflammatory response and cognitive impairment via PI3K/AKT/FoxO3a signaling pathway in Alzheimer's disease mice, Aging 12 (20) (2020) 20862–20879.

[79] J. Zhang, Y. Zheng, Y. Luo, Y. Du, X. Zhang, J. Fu, Curcumin inhibits LPS-induced neuroinflammation by promoting microglial M2 polarization via TREM2/ TLR4/ NF-κB pathways in BV2 cells, Mol. Immunol. 116 (2019) 29–37.

[80] K. Takahashi, M. Prinz, M. Stagi, O. Chechneva, H. Neumann, TREM2-transduced myeloid precursors mediate nervous tissue debris clearance and facilitate recovery in an animal model of multiple sclerosis, PLoS Med. 4 (4) (2007), e124.

[81] C. Li, B. Zhao, C. Lin, Z. Gong, X. An, TREM2 inhibits inflammatory responses in mouse microglia by suppressing the PI3K/NF-κB signaling, Cell Biol. Int. 43 (4) (2019) 360–372.

[82] Z. Qiu, H. Wang, M. Qu, S. Zhu, H. Zhang, Q. Liao, C. Miao, Consecutive Injection of High-Dose Lipopolysaccharide Modulates Microglia Polarization via TREM2 to Alter Status of Septic Mice, Brain Sci. 13 (1) (2023).

[83] Q. Luo, D. Deng, Y. Li, H. Shi, J. Zhao, Q. Qian, W. Wang, J. Cai, W. Yu, J. Liu, TREM2 insufficiency protects against pulmonary fibrosis by inhibiting m2 macrophage polarization, Int Immunopharmacol. 118 (2023), 110070.

[84] X.X. Fu, S.Y. Chen, H.W. Lian, Y. Deng, R. Duan, Y.D. Zhang, T. Jiang, The TREM2 H157Y variant influences microglial phagocytosis, polarization, and inflammatory cytokine release, Brain Sci. 13 (4) (2023).

[85] M. Wu, M. Liao, R. Huang, C. Chen, T. Tian, H. Wang, J. Li, J. Li, Y. Sun, C. Wu, Q. Li, X. Xiao, Hippocampal overexpression of TREM2 ameliorates high fat diet induced cognitive impairment and modulates phenotypic polarization of the microglia, Genes Dis. 9 (2) (2022) 401–414.

[86] Y. Hu, C. Li, X. Wang, W. Chen, Y. Qian, X. Dai, TREM2, driving the microglial polarization, Has a TLR4 sensitivity profile after subarachnoid hemorrhage, Front Cell Dev. Biol. 9 (2021), 693342.

[87] H. Keren-Shaul, A. Spinrad, A. Weiner, O. Matcovitch-Natan, R. Dvir-Szternfeld, T.K. Ulland, E. David, K. Baruch, D. Lara-Astaiso, B. Toth, S. Itzkovitz, M. Colonna, M. Schwartz, I. Amit, A unique microglia type associated with restricting development of Alzheimer's disease, Cell 169 (7) (2017), 1276-1290. e17.

[88] H. Zhu, Q. Gui, X. Hui, X. Wang, J. Jiang, L. Ding, X. Sun, Y. Wang, H. Chen, TGF-β1/Smad3 signaling pathway suppresses cell apoptosis in cerebral ischemic stroke rats, Med Sci. Monit. 23 (2017) 366–376.

[89] S.Y. Cheon, K.J.Jomm Cho, Lipid Metab., Inflamm., Foam Cell Form. Health Metab. Disord.: Target. mTORC1 99 (11) (2021) 1497–1509.

[90] B.C. Farmer, A.E. Walsh, J.C. Kluemper, L.A.J.Fin Johnson, Lipid droplets Neurodegener. Disord. 14 (2020) 742.

[91] J. Marschallinger, T. Iram, M. Zardeneta, S.E. Lee, B. Lehallier, M.S. Haney, J. V. Pluvinage, V. Mathur, O. Hahn, D.W. Morgens, J. Kim, J. Tevini, T.K. Felder, H. Wolinski, C.R. Bertozzi, M.C. Bassik, L. Aigner, T. Wyss-Coray, Lipid-droplet-accumulating microglia represent a dysfunctional and proinflammatory state in the aging brain, Nat. Neurosci. 23 (2) (2020) 194–208.

[92] R.Y. Li, Q. Qin, H.C. Yang, Y.Y. Wang, Y.X. Mi, Y.S. Yin, M. Wang, C.J. Yu, Y. Tang, TREM2 in the pathogenesis of AD: a lipid metabolism regulator and potential metabolic therapeutic target, Mol. Neurodegener. 17 (1) (2022) 40.

[93] Y. Guo, X. Wei, H. Yan, Y. Qin, S. Yan, J. Liu, Y. Zhao, F. Jiang, H. Lou, TREM2 deficiency aggravates α-synuclein-induced neurodegeneration and neuroinflammation in Parkinson's disease models, Faseb J. 33 (11) (2019) 12164–12174.

[94] T.H. Do, F. Ma, P.R. Andrade, R. Teles, B.J. de Andrade Silva, C. Hu, A. Espinoza, J.E. Hsu, C.S. Cho, M. Kim, J. Xi, X. Xing, O. Plazyo, L.C. Tsoi, C. Cheng, J. Kim, B. D. Bryson, A.M. O'Neill, M. Colonna, J.E. Gudjonsson, E. Klechevsky, J.H. Lee, R. L. Gallo, B.R. Bloom, M. Pellegrini, R.L. Modlin, TREM2 macrophages induced by human lipids drive inflammation in acne lesions, Sci. Immunol. 7 (73) (2022), eabo2787.

[95] J.A. van Diepen, J.F. Berbée, L.M. Havekes, P.C. Rensen, Interactions between inflammation and lipid metabolism: relevance for efficacy of anti-inflammatory drugs in the treatment of atherosclerosis, Atherosclerosis 228 (2) (2013) 306–315.

[96] T.K. Ulland, W.M. Song, S.C. Huang, J.D. Ulrich, A. Sergushichev, W.L. Beatty, A. A. Loboda, Y. Zhou, N.J. Cairns, A. Kambal, E. Loginicheva, S. Gilfillan, M. Cella, H.W. Virgin, E.R. Unanue, Y. Wang, M.N. Artyomov, D.M. Holtzman, M. Colonna, TREM2 Maintains Microglial Metabolic Fitness in Alzheimer's Disease, Cell 170 (4) (2017), 649-663.e13.

[97] L. Zhong, X.F. Chen, The emerging roles and therapeutic potential of soluble TREM2 in Alzheimer's disease, Front. Aging Neurosci. 11 (2019) 328.

[98] P. Zhao, Y. Xu, L. Jiang, X. Fan, L. Li, X. Li, H. Arase, Y. Zhao, W. Cao, H. Zheng, H. Xu, Q. Tong, N. Zhang, Z. An, A tetravalent TREM2 agonistic antibody reduced amyloid pathology in a mouse model of Alzheimer's disease, Sci. Transl. Med. 14 (661) (2022), eabq0095.

[99] H. Zheng, B. Cheng, Y. Li, X. Li, X. Chen, Y.W. Zhang, TREM2 in Alzheimer's disease: microglial survival and energy metabolism, Front. Aging Neurosci. 10 (2018), 395.

[100] S. Wang, M. Mustafa, C.M. Yuede, S.V. Salazar, P. Kong, H. Long, M. Ward, O. Siddiqui, R. Paul, S. Gilfillan, A. Ibrahim, H. Rhinn, I. Tassi, A. Rosenthal, T. Schwabe, M. Colonna, Anti-human TREM2 induces microglia proliferation and reduces pathology in an Alzheimer's disease model, J. Exp. Med. 217 (9) (2020).

[101] A. Dabla, Y.C. Liang, N. Rajabalee, C. Irwin, C.G.J. Moonen, J.V. Willis, S. Berton, J. Sun, TREM2 promotes immune evasion by mycobacterium tuberculosis in human macrophages, mBio 13 (4) (2022), e0145622.